

# Dimerization and Stacking in Transition-Metal Bisdithiolenes and Tetrathiulates

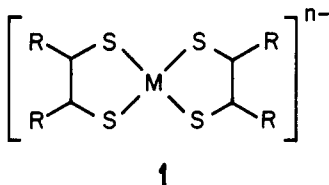
Santiago Alvarez,\*† Ramón Vicente,† and Roald Hoffmann\*‡

Contribution from the Facultat de Química, Universitat de Barcelona, Diagonal, 647 Barcelona-08028, and the Department of Chemistry, Cornell University, Ithaca, New York 14853. Received December 18, 1984

**Abstract:** The structural, chemical, and electrical properties of a number of transition-metal bisdithiolenes and tetrathiolenes are studied through qualitative MO and band structure calculations. The formation of metal-metal- or metal-sulfur-bonded dimers of bisdithiolenes is found to depend on a delicate balance of several factors: sulfur lone-pair repulsion between the monomers, size and occupation of the transition metal's d orbitals, and steric repulsions between substituents in the dithiolenes ligands. Regular stacks of transition-metal bisdithiolenes are predicted to be unstable toward Peierls distortions for integral oxidation states. The sulfur lone-pair repulsions are responsible for the slippage of the stacks as well as for the sliding of neighboring stacks, giving rise to triclinic crystals. The resulting stacking pattern can produce mixing of the  $\sigma$  and  $\pi$  sulfur lone pairs, hence two dimensionality in the electrical conductivity. An isolobal analogy allows one formally to replace carbon-carbon double bonds by a metal atom, providing the orbital foundation of a structural and electrical analogy between transition-metal bisdithiolenes and tetrathiofulvalene derivatives. The coordinative ability of the simplest tetrathiolene, ethylenetetrathiolate (ett), is analyzed. Of the two coordination modes available for this ligand, the dithiolene-like mode is found to be more stable than the dithiocarbamate-like one both for discrete and polymeric compounds. But the dithiocarbamate coordination mode should be accessible. A likely structural candidate for the polymers  $M(\text{ett})$  is a planar ribbon; a band composed of the metal  $d_{xz}$  and a ligand  $\pi$  orbital shows dispersion due to through-bond coupling and could account for one-dimensional electrical conductivity. Alternative one- and two-dimensional structures for the as yet unknown compounds  $M_2(\text{ett})$  and  $M_3(\text{ett})$  are also studied.

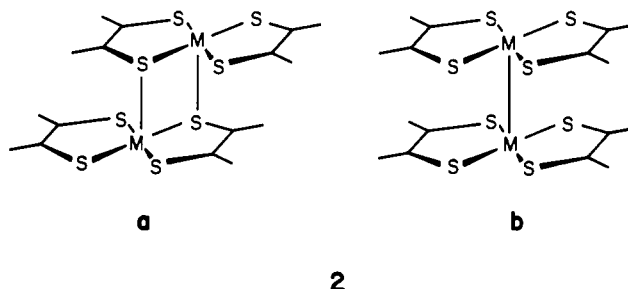
While much has been learned about transition-metal dithiolenes,<sup>1</sup> an interesting remaining intellectual challenge is the attainment of that degree of the understanding of their structural and electronic properties that could give rise to the design and synthesis of low-dimensional materials with metallic or semi-conducting properties. The mode of association of metal dithiolenes is the subject of this work.

The metal bisdithiolenes **1** ( $R = \text{H}, \text{CN}, \text{CF}_3$ , and  $\text{Ph}$ ;  $n = 0, 1$ , and  $2$ ) are planar compounds which may appear in the crystal state as isolated units,<sup>2</sup> as dimers with metal-sulfur bonds,<sup>2d,3,4</sup>



**1**

**2a**, metal-metal bonded dimers,<sup>5</sup> **2b**, or as partially oxidized stacks featuring metal-metal bonds and different degrees of pairing distortion.<sup>6</sup> Much less is known about the analogous compounds



with one<sup>7</sup> or two<sup>8</sup> selenium atoms replacing the donor sulfur atoms

\*Universitat de Barcelona.

†Cornell University.

(1) (a) Burns, R. P.; McAuliffe, C. A. *Adv. Inorg. Chem. Radiochem.* **1979**, *22*, 303. (b) Ibers, J. A.; Pace, L. J.; Martinsen, J.; Hoffman, B. M. *Struct. Bonding (Berlin)* **1982**, *50*, 1. (c) Hoyer, E.; Dietzsch, W.; Schroth, W. *Z. Chem.* **1971**, *11*, 41. (d) Eisenberg, R.; *Prog. Inorg. Chem.* **1970**, *12*, 295. (e) Coucouvanis, D. *Prog. Inorg. Chem.* **1970**, *11*, 233. (f) Schrauzer, G. N. *Acc. Chem. Res.* **1969**, *2*, 72. (g) Lindoy, L. F. *Coord. Chem. Rev.* **1969**, *4*, 41. (h) McCleverty, J. A. *Prog. Inorg. Chem.* **1968**, *10*, 49. (i) Alcácer, L.; Novais, H. In "Extended Linear Chain Compounds"; Miller, J. S., Ed.; Plenum Press: New York, 1983; Vol. 3, Chapter 6.

(2) (a) Mahadevan, C.; Seshasayee, M.; Murthy, B. V. R.; Kuppusamy, P.; Manoharan, P. T. *Acta Crystallogr., Sect. C* **1983**, *C39*, 1335. (b) Dessy, G.; Fares, V.; Bellitto, C.; Flamini, A. *Cryst. Struct. Commun.* **1982**, *11*, 1743. (c) Manoharan, P. T.; Noordik, J. H.; deBoer, E.; Keijzers, C. *J. Chem. Phys.* **1981**, *74*, 1980. (d) Kobayashi, A.; Sasaki, Y. *Bull. Chem. Soc. Jpn.* **1977**, *50*, 2650. Plumlee, K. W.; Hoffman, B. M.; Ibers, J. A.; Zoos, Z. G. *J. Chem. Phys.* **1975**, *63*, 1926. (f) Hove, M. J.; Hoffman, B. M.; Ibers, J. A. *J. Chem. Phys.* **1972**, *56*, 3490. (g) Enemark, J. H.; Ibers, J. A. *Inorg. Chem.* **1968**, *7*, 2636. (h) Forrester, J. D.; Zalkin, A.; Templeton, D. H. *Inorg. Chem.* **1964**, *3*, 1507. (i) Fritchie, C. J. *Acta Crystallogr.* **1966**, *20*, 107. (j) Forrester, J. D.; Zalkin, A.; Templeton, D. H. *Inorg. Chem.* **1964**, *3*, 1500. (k) Cassoux, P.; Interrante, L.; Wasper, J. *Mol. Cryst. Liq. Cryst.* **1982**, *81*, 293-300. (l) Lindqvist, O.; Sjölin, L.; Sieler, J.; Steimecke, G.; Hoyer, E. *Acta Chem. Scand., Ser. A* **1979**, *A33*, 445. (m) Kasper, J. S.; Interrante, L. V.; Secaur, C. A. *J. Am. Chem. Soc.* **1975**, *97*, 890-891. (n) Lindqvist, O.; Andersen, L.; Sieler, Y.; Steimecke, G.; Hoyer, E. *Acta Chem. Scand., Ser. A* **1982**, *A36*, 855. (o) Lindqvist, O.; Sjölin, L.; Sieler, Y.; Steimecke, G.; Hoyer, E. *Acta Chem. Scand., Ser. A* **1982**, *A36*, 853. (p) Sartain, D.; Truter, M. *J. Chem. Soc. A* **1967**, 1264. (q) Henkel, G.; Greiwe, K.; Krebs, B. *Angew. Chem., Int. Ed. Engl.* **1985**, *24*, 117.

(3) (a) Kanatzidis, M. G.; Coucouvanis, D. *Inorg. Chem.* **1984**, *23*, 403. (b) Snow, M. R.; Ibers, J. A. *Inorg. Chem.* **1973**, *12*, 249. (c) Baker-Hawkes, M. J.; Dori, Z.; Eisenberg, R.; Gray, H. B. *J. Am. Chem. Soc.* **1968**, *90*, 4253. (d) Hamilton, W. C.; Bernal, I. *Inorg. Chem.* **1967**, *6*, 2003. (e) Enemark, J. H.; Lipscomb, W. N. *Inorg. Chem.* **1965**, *4*, 1729. (f) Christou, G.; Huffman, J. C. *J. Chem. Soc., Chem. Commun.* **1983**, 558. (g) Dorfman, J. R.; Rao, Ch.P.; Holm, R. H. *Inorg. Chem.* **1985**, *24*, 453.

(4) A related compound is that formed from  $(\eta^5\text{-C}_5\text{H}_5)_2\text{Co}(\text{S}_2\text{C}_6\text{H}_4)$  in a solid-state dimerization: Miller, E. J.; Brill, T. B.; Rheingold, A. L.; Fultz, W. C. *J. Am. Chem. Soc.* **1983**, *105*, 7580.

(5) Browall, K. W.; Bursh, T.; Interrante, L. V.; Kasper, J. S. *Inorg. Chem.* **1972**, *11*, 1800. Browall, K. W.; Interrante, L. V.; Kasper, J. S. *J. Am. Chem. Soc.* **1971**, *93*, 6289.

(6) (a) Ahmad, M. M.; Turner, J. D.; Underhill, A. E.; Kobayashi, A.; Sasaki, Y.; Kobayashi, H. *J. Chem. Soc., Dalton Trans.* **1984**, 1759. (b) Ahmad, M. M.; Turner, D. J.; Underhill, A. E.; Jacobsen, C. S.; Mortensen, K.; Carneiro, K. *Phys. Rev. B* **1984**, *29*, 4796. (c) Kobayashi, A.; Sasaki, Y.; Kobayashi, H.; Underhill, A. E.; Ahmad, M. M., unpublished results. (d) Kobayashi, A.; Sasaki, Y.; Kobayashi, H.; Underhill, A. E.; Ahmad, M. M. *J. Chem. Soc., Chem. Commun.* **1982**, 390. (e) Alcácer, L. J.; Novais, H.; Pedroso, F.; Flandrois, S.; Coulon, C.; Chasseau, D.; Gaultier, J. *Solid State Commun.* **1980**, *35*, 945. (f) Valade, L.; Bousseau, M.; Gleizes, A.; Cassoux, P. *J. Chem. Soc., Chem. Commun.* **1983**, 110. (g) Bousseau, M.; Valade, L.; Bruniquel, M.-F.; Cassoux, P.; Garbouskas, M.; Interrante, L.; Kasper, J. *Nouv. J. Chim.* **1984**, *8*, 3. (h) Kobayashi, A.; Mori, T.; Sasaki, Y.; Kobayashi, H.; Ahmad, M. M.; Underhill, A. E. *Bull. Chem. Soc. Jpn.* **1984**, *57*, 3262. (i) Cassoux, P.; Valade, P.; Bousseau, M.; Legros, J.-P.; Garbouskas, M.; Interrante, L. *Proc. Abano-Terme Conf.* June **1984**, 1.

(7) Pierpont, C. G.; Corden, B. J.; Eisenberg, R. *J. Chem. Soc., Chem. Commun.* **1969**, 401.

**Table I.** Structural Properties of Associated Dithiolenes,  $A_x[M(S_2C_2R_2)_2]^{n-}$ 

| M  | A                           | R  | d <sup>n</sup> | type of assoc       | M-S (or M-M) dist | pyramidaliz,° Å | ref  |
|----|-----------------------------|--|----------------|---------------------|-------------------|-----------------|------|
| Fe | Ph <sub>4</sub> P           | COOCH <sub>3</sub>                               | 5              | M-S dimer           | 2.466             | 0.434           | 3a   |
| Fe | <i>n</i> -Bu <sub>4</sub> N | CN   | 5              | M-S dimer           | 2.46              | 0.36            | 3d   |
| Co |                             | CF <sub>3</sub>                                  | 5              | M-S dimer           | 2.38              | 0.37            | 3e   |
| Co | <i>n</i> -Bu <sub>4</sub> N | (C <sub>4</sub> Cl <sub>2</sub> ) <sub>1/2</sub> | 6              | M-S dimer           | 2.404             | 0.26            | 3c   |
| Pd |                             | H  | 6              | M-M dimer           | 2.790             | 0.12            | 5    |
| Pt |                             | H  | 6              | M-M dimer           | 2.748             | 0.16            | 5    |
| Ni | <i>n</i> -Bu <sub>4</sub> N | (CS <sub>3</sub> ) <sub>1/2</sub>                | 6.3            | M-M slipped stack   |                   | 0               | 6f   |
| Ni | (TTF) <sub>0.5</sub>        | (CS <sub>3</sub> ) <sub>1/2</sub>                | 6.5            | M-M slipped stack   | 3.55              | 0               | 6g   |
| Pt | Li <sub>0.5</sub>           | CN   | 6.5            | M-M irregular stack | 3.346             | 0               | 6a   |
|    |                             |  |                |                     | 3.987             |                 |      |
|    |                             |  |                |                     | 4.298             |                 |      |
| Pt | Li <sub>0.82</sub>          | CN   | 6.8            | M-M stack           | 3.639             | 0               | 6d,h |
| Ni | Ph <sub>3</sub> MeP         | CN   | 7              | M-S "dimer"         | 3.591             |                 | 2i   |
|    |                             |  |                |                     | 3.708             |                 |      |
| Ni | Et <sub>4</sub> N           | CN   | 7              | M-S "dimer"         | 3.52              |                 | 2d   |
| Pt | Rb                          | CN   | 7              | M-M "dimer"         | 3.356             |                 | 6a   |
|    |                             |  |                |                     | 3.512             |                 |      |
| Cu | PClPh <sub>3</sub>          | CN   | 8              | M-M "dimer"         | 4.02              |                 | 2h   |
|    |                             |  |                |                     | 4.43              |                 |      |
| Au | PClPh <sub>3</sub>          | CF <sub>3</sub>                                  | 8              | M-S "dimer"         | 3.96              |                 | 2g   |

<sup>a</sup>The height of the M atom above the mean plane of the sulfurs.

in the ligand. A summary of the structural properties of these dimers and stacks is presented in Table I.

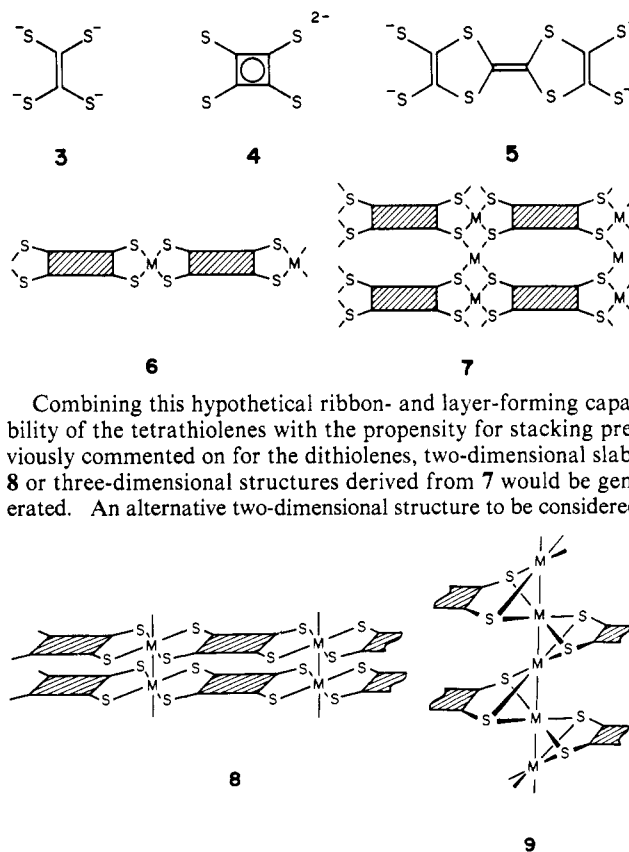
Some general trends can be detected: (a) No association occurs for d<sup>8</sup> and d<sup>9</sup> systems<sup>2</sup> (these are not represented in Table I). (b) Weak interactions exist for d<sup>7</sup> compounds: M-S contacts (~3.5 Å) for Ni but M-M approaches (3.36 Å) for Pt. (c) Dimers are formed for d<sup>5</sup> and d<sup>6</sup> compounds, M-S bonded for Fe and Co (2.4–2.5 Å) but M-M bonded for Pd and Pt (2.7–2.8 Å). (d) First-row transition metals experience larger out-of-plane displacements (0.26–0.43 Å) than second- and third-row transition metals (0.12–0.16 Å).

As far as the electrical and magnetic properties are concerned, a large number of weakly associated dithiolenes show sizeable antiferromagnetic interaction,<sup>2a,3b,9</sup> a typical value of the coupling constant *J* being of the order of ~500 cm<sup>-1</sup>. In accord with the weak interactions associated with the antiferromagnetism of these compounds, they are semiconductors with room-temperature electrical conductivities in the range 10<sup>-5</sup>–10<sup>-11</sup> Ω<sup>-1</sup> cm<sup>-1</sup> and conductivity gaps from 0.2 to 3.0 eV.<sup>2d,j,9a,d,10</sup> Although some reach conductivities of about 10<sup>-2</sup> Ω<sup>-1</sup> cm<sup>-1</sup>, this happens only in cases in which the anionic dithiolene coexists in the crystal with organic donors such as tetrathiofulvalene (TTF) or perylene<sup>1i,9a,11</sup> or when the counteranion is Cu<sup>2+</sup>.<sup>10k</sup> So far we can conclude that the metal bisdithiolenes themselves have electrical conductivities

at room temperature smaller than 10<sup>-5</sup> Ω<sup>-1</sup> cm<sup>-1</sup>, no matter what the central metal is and which is its oxidation state; larger conductivity appears only when a counteranion may play a role in the transport properties.

There are, however, a few metal bisdithiolenes with metallic conductivity, i.e., the conductivity is not thermally activated and typical values are in the range 10 < σ<sub>RT</sub> < 1000 Ω<sup>-1</sup> cm<sup>-1</sup>. One case is a salt in which the polyene cations form stacks and are probably responsible for the conducting behavior.<sup>6e,10c</sup> The other group of compounds is the partially reduced salts of lithium and rubidium prepared by Underhill and co-workers,<sup>6a-c</sup> whose structures have already been noted (Table I, bottom).

If the dithiolate is replaced by a tetrathiolate such as ethylenetetrathiolate (ett) **3**, tetrathiosquarate (ttsq) **4**, or tetrathiofulvalenetetrathiolate (tftf), **5**, a ribbon could be formed as in **6**, but also two dimensional layers as in **7**.



(8) (a) Davison, A.; Shawl, E. T. *Inorg. Chem.* **1970**, *9*, 1820. (b) Sandman, D. J.; Stark, J. C.; Acampora, L. A.; Samuelson, L. A.; Allen, G. W.; Jansen, S.; Jones, M. T.; Foxman, B. M. *Mol. Cryst. Liq. Cryst.* **1984**, *107*, 1. (c) Hever, W. B.; Hoffman, B. M., 190th ACS National Meeting, Chicago, September 1985.

(9) (a) Interrante, L. V.; Browall, K. W.; Hart, H. R.; Jacobs, I. S.; Watkins, G. D.; Lee, S. H. *J. Am. Chem. Soc.* **1975**, *97*, 889. (b) Weiher, J. F.; Melby, L. R.; Benson, R. E. *J. Am. Chem. Soc.* **1964**, *86*, 4329. (c) Dance, I. G. *Inorg. Chem.* **1973**, *12*, 2748. (d) Isett, L. C.; Rosso, D. M.; Bottger, G. L. *Phys. Rev. B* **1980**, *B22*, 4739.

(10) (a) Ahmad, M. M.; Underhill, A. E. *J. Chem. Soc., Dalton Trans.* **1983**, 165. (b) Wheland, R. C.; Gillson, J. L. *J. Am. Chem. Soc.* **1976**, *98*, 3916. (c) Alcácer, L. J.; Maki, A. H. *J. Phys. Chem.* **1974**, *78*, 215. (d) Pérez-Albuerne, N. A.; Isett, L. C.; Haller, R. W. *J. Chem. Soc., Chem. Commun.* **1977**, 417. (e) Interrante, L. V.; Bray, J. W.; Hart, H. R.; Kasper, J. S.; Piacente, P. A. *J. Am. Chem. Soc.* **1977**, *99*, 3523. (f) Browall, K. W.; Interrante, L. V. *J. Coord. Chem.* **1973**, *3*, 27. (g) Plumlee, K. W.; Hoffman, B. M.; Ratajack, M. T.; Kannewurf, C. R. *Solid State Commun.* **1974**, *15*, 1651. (h) Miller, J. S.; Epstein, A. J. *J. Coord. Chem.* **1979**, *8*, 191. (i) Miles, M. G.; Wilson, J. D. *Inorg. Chem.* **1975**, *14*, 2357. (j) Fendley, J. J.; Jonscher, A. K. *J. Chem. Soc., Faraday Trans. 1* **1973**, *69*, 1213. (k) Manecke, G.; Wöhrle, D. *Makromol. Chem.* **1968**, *116*, 36. (l) Rosseinsky, D. R.; Malpas, R. E. *J. Chem. Soc., Dalton Trans.* **1979**, 749. (m) Papavassiliou, G. C. *Z. Naturforsch., B* **1982**, *37B*, 825.

(11) (a) Alcácer, L.; Maki, A. H. *J. Phys. Chem.* **1974**, *78*, 215. (b) Alcácer, L.; Maki, A. H. *J. Phys. Chem.* **1976**, *80*, 1912. (c) Wudl, F.; Ho, C. H.; Nagel, A. *J. Chem. Soc., Chem. Commun.* **1973**, 923. (d) Calas, P.; Fabre, J. M.; Khalife-El-Saleh; Mas, A.; Torrelles, E.; Giral, L. *Tetrahedron Lett.* **1975**, 4475.

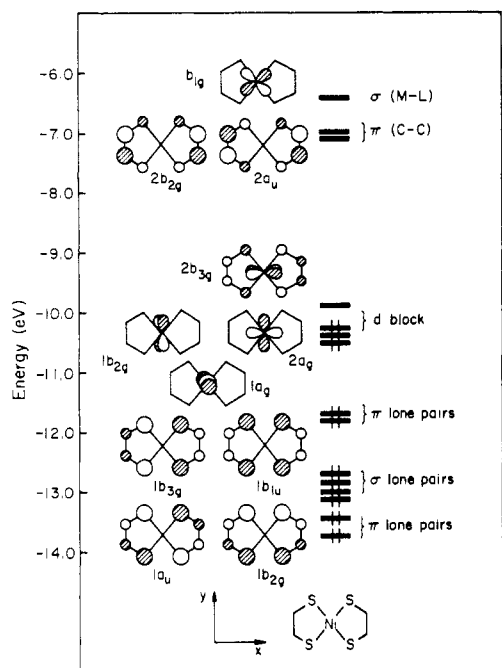


Figure 1. Molecular orbital diagram of  $[\text{Ni}(\text{S}_2\text{C}_2\text{H}_2)_2]$ .

is **9**, related to known molecular compounds in which an  $\text{M}_2\text{L}_{2n}$  fragment with or without metal-metal bonds is bound to two sulfur atoms of a dithiolene or tetrathiolene with the M-M vector perpendicular to the plane of the ligand;<sup>12</sup> similar compounds exist with the  $\text{MS}_4$  moiety (M = Ni, Pd, and Pt) occupying the place of the tetrathiolene ligand.<sup>7</sup>

Understanding of the electronic structure of these compounds should allow an interpretation of their structural diversity and permit predictions of the structures of as yet unknown compounds. We would like to start with the study of the discrete molecules and move stepwise toward dimers and polymers. The parameters and structural data used for our extended Hückel calculations are specified in the Appendix section.

#### Molecular Orbitals of the Metal Bisdithiolenes

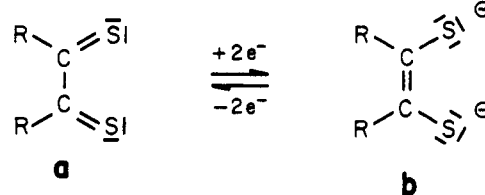
A number of MO calculations on metal bisdithiolenes have been reported.<sup>13</sup> However, the level order in the valence region varies from one calculation to another, and a short discussion is imperative in order to calibrate our calculations against the experimental information.

The MO diagram for  $\text{Ni}(\text{edt})_2$  (edt = ethylenedithiolate, **1**, R = H), shown in Figure 1, presents the usual pattern for square-

planar transition-metal complexes with one ( $b_{1g}$ ) above four d orbitals. One of them ( $d_{x^2}$ ) interacts with the  $b_{3g}(\pi)$  orbital of the  $\pi$ -donor ligands, thus opening a gap, a small one, but large enough to account for the diamagnetism and low-energy absorption band of  $\text{Ni}(\text{edt})_2$ <sup>13a</sup> and related  $d^6$  compounds<sup>1h,14</sup> and in agreement with the  ${}^2B_{3g}$  ground state found in the ESR of  $d^7$  compounds  $\text{M}(\text{mnt})_2^-$  (**1**, R = CN; M = Ni, Pd, and Pt).<sup>15</sup> For a less electronegative metal like Mn, the metal-sulfur  $b_{3g}(\pi)$  interaction should be poorer, hence the gap smaller and a high-spin configuration is found.<sup>2a</sup> Below the d block is a group of four orbitals of  $\pi$  symmetry interspersed with a block of four lone pairs of  $\sigma$  symmetry primarily localized on S. Two further  $\pi$  orbitals are at still lower energy and are not shown in Figure 1.

We specified a d-electron count above,  $d^7$  in  $\text{Ni}(\text{mnt})_2^-$ . This is a dangerous step in any discussion of transition-metal dithiolenes, and we had better face up immediately to the ambiguities of electron counting and oxidation state in this field.

Dithiolenes are noninnocent ligands. They could be viewed as neutral **10a** or dianionic **10b**. The two extremes differ in the number of  $\pi$  electrons: the neutral form has four  $\pi$  electrons and the dianionic six. Either extreme has four sulfur  $\sigma$  lone pairs.



#### 10

If one adopts the neutral formalism,  $\text{Ni}(\text{mnt})_2^-$  would be  $\text{Ni}(-\text{I})$ , " $d^{11}$ ", while with the dithiolene dianionic we would reach  $\text{Ni}(\text{I})$ ,  $d^9$ .

Let us look into the metal bisdithiolene electronic structure in detail to see what it tells us. Making no judgment as to electron count, the dithiolene unit bears four  $\pi$  orbitals, butadienoid in character. These are shown in **11**. For two dithiolene units, these are doubled as symmetric and antisymmetric combinations,  $\chi_{nA} \pm \chi_{nB}$ , where A is one dithiolene, and B the other one.

We can find these in Figure 1. The lowest combinations are not in the figure. But the next  $\pi$  orbitals  $1a_u + 1b_{2g}$  are  $\chi_{2A} - \chi_{2B}$  and  $\chi_{2A} + \chi_{2B}$ , respectively. And above them are  $1b_{3g}$  and  $1b_{1u}$ ,  $\chi_{3A} - \chi_{3B}$  and  $\chi_{3A} + \chi_{3B}$ , respectively.  $\chi_{4A} \pm \chi_{4B}$  are unfilled, near the top of the figure. Clearly the electronic structure of the metal bisdithiolene is telling us that there are three mainly dithiolene-based  $\pi$  orbitals filled per dithiolene. This is consistent with a dianionic dithiolene resonance structure, **10b**.

Another approach to specifying the electron count is to actually extract from a fragment MO analysis the population of the fragment dithiolene  $\pi$  orbitals in the complex. The numbers we obtain are  $\chi_1$  1.98,  $\chi_2$  2.00,  $\chi_3$  1.72, and  $\chi_4$  0.02.

While these observations favor the dianionic dithiolene formulation, we should keep in mind the essential ambiguity of any oxidation-state formalism. Furthermore, there may be substantial variation in the role of the various resonance forms as the metal and total molecular charge vary.

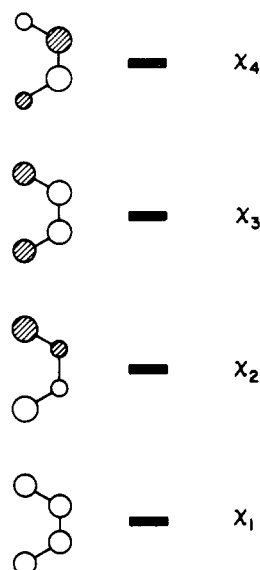
Another perspective on the dithiolene orbitals may be mentioned here. Given that the dithiolene ligand in the complex is best described as dianionic, we can go further toward resonance structure **10b** by identifying certain orbitals as S lone pairs or the ethylene  $\pi$  bond. Such an identification must be an approximation,

(14) Notice that we consider each dithiolene ligand  $\text{R}_2\text{C}_2\text{S}_2$  as dianionic for electron accounting purposes. We will turn to the analysis of this formalism later in the body of the paper.

(15) (a) Schmitt, R. D.; Maki, A. H. *J. Am. Chem. Soc.* **1968**, *90*, 2288. (b) Kirmse, R.; Dietzsch, W. J. *J. Inorg. Nucl. Chem.* **1976**, *38*, 255. (c) Kirmse, R.; Dietzsch, W. J. *Z. Chem.* **1977**, *17*, 33. (d) Kirmse, R.; Dietzsch, W. J.; Solov'ev, B. *J. Inorg. Nucl. Chem.* **1976**, *39*, 1157.

(12) (a) Broadhurst, P. V.; Johnson, B. F. G.; Lewis, J.; Raithby, P. R. *J. Chem. Soc., Chem. Commun.* **1982**, 140. (b) Teo, B. K.; Bakirtzis, V.; Snyder-Robinson, P. A. *J. Am. Chem. Soc.* **1983**, *105*, 6330. (c) Weber, H. P.; Bryan, R. F. *J. Chem. Soc. A* **1967**, 182; *J. Chem. Soc., Chem. Commun.* **1966**, 329. (d) Shaver, A.; Fitzpatrick, P. J.; Steliou, K.; Butler, I. S. *J. Organomet. Chem.* **1979**, *172*, C59. (e) Shaver, A.; Fitzpatrick, P. J.; Steliou, K.; Butler, I. S. *J. Am. Chem. Soc.* **1979**, *101*, 1313. (f) Nöth, V. H.; Schuchardt, U. *Z. Anorg. Allg. Chem.* **1975**, *418*, 97. (g) Bolinger, C. M.; Raufuss, B.; Rheingold, A. L. *J. Am. Chem. Soc.* **1983**, *105*, 6321. (h) Dorfman, J. R.; Holm, R. H. *Inorg. Chem.* **1983**, *22*, 3179. (i) Szeymies, D.; Krebs, B.; Henkel, G. *Angew. Chem. Suppl.* **1983**, 1176. (j) Miller, W. K.; Haltiwanger, R. C.; Van Derveer, M. C.; Rakowski DuBois, M. *Inorg. Chem.* **1983**, *22*, 2973. (k) Rakowski DuBois, M.; Haltiwanger, R. C.; Miller, D. J.; Glatzmeier, G. *J. Am. Chem. Soc.* **1979**, *101*, 5245. (l) McKenna, M.; Wright, L. L.; Miller, D. J.; Tanner, L.; Haltiwanger, R. C.; Rakowski DuBois, M. *J. Am. Chem. Soc.* **1983**, *105*, 5329. (m) Higgins, R. W.; Huffman, J. C.; Christou, G. *J. Chem. Soc., Chem. Commun.* **1983**, 1313. (n) Bosman, W. P.; van der Linden, H. G. M. *J. Chem. Soc., Chem. Commun.* **1977**, 714.

(13) (a) Schrauzer, G. N.; Mayweg, V. P. *J. Am. Chem. Soc.* **1965**, *87*, 3585. (b) Shupack, S. I.; Billig, E.; Clark, R. J. H.; Williams, R.; Gray, H. B. *J. Am. Chem. Soc.* **1964**, *86*, 4594. (c) Sano, M.; Adachi, H.; Yamatera, H. *Bull. Chem. Soc. Jpn.* **1981**, *54*, 2636. (d) Blomberg, M. R. A.; Wahlgren, U. *Chem. Phys.* **1980**, *49*, 117. (e) Ciullo, G.; Sgamellotti, A. *Z. Phys. Chem. N.F.* **1976**, *100*, 83. (f) Zális, S.; Vlček, A. A. *Inorg. Chim. Acta* **1982**, *58*, 89. (g) Demoulin, D.; Fischer-Hjalmar, I.; Henriksson-Enflo, A.; Pappas, J. A.; Sundbom, M. *Int. J. Quantum Chem.* **1977**, *16*, 1. (h) Fischer-Hjalmar, I.; Henriksson-Enflo, A. *Adv. Quantum Chem.* **1982**, *16*, 1.



## 11

because the lone pairs and CC  $\pi$  and  $\pi^*$  must mix, resulting in the butadienoid orbitals of **11**. It turns out that  $\chi_1$  is 54% on the two sulfurs,  $\chi_2$  89%,  $\chi_3$  46%. Clearly it is appropriate to call  $\chi_2$  a S lone pair combination, the antisymmetric one. But both  $\chi_1$  and  $\chi_3$  have ethylene  $\pi$  as well as S lone-pair contributions, in approximately equal amounts. Mixing of these two semilocalized orbitals is substantial. Being fully aware of the necessary delocalization, we will nevertheless occasionally refer to  $\chi_3$ , for reasons of convenience, as the symmetric S lone-pair combination.

Let us return to the experimental evidence for the level scheme of Figure 1. The vibrational spectra of the  $\text{Ni}(\text{R}_2\text{C}_2\text{S}_2)_2^{n-}$  series ( $n = 0, 1, \text{ and } 2$ ) show an increase in the C=C force constants and a decrease in the C-S and Ni-S force constants on going from  $n = 0$  ( $d^6$ ) to  $n = 2$  ( $d^8$ ).<sup>16</sup> This is in excellent agreement with the C-C bonding and C-S and Ni-S antibonding character of the  $2b_{3g}$  orbital which is increasingly filled along this series. The Ni-S antibonding nature of the LUMO is further confirmed by the experimental average Ni-S bond distances: 2.101 for  $n = 0$ ;<sup>17</sup> 2.143 for  $n = 1$ ;<sup>2a,c,d,i,18</sup> and 2.171 for  $n = 2$ .<sup>2d,f,19</sup>

It must be mentioned that the experimental evidence suggests larger contribution of the sulfur  $\pi$  lone-pair orbital  $\chi_{3A} - \chi_{3B}$  to  $2b_{3g}$  than found in our calculations. This must be a consequence of our approximate theoretical method or parameter choice, but the disagreement is only quantitative and does not invalidate our qualitative results.

Additional electrochemical reduction can produce  $[\text{M}(\text{mnt})_2]^{3-}$  ( $\text{M} = \text{Ni}$  and  $\text{Pd}$ ), and ESR results indicate that the unpaired electron is localized mainly in the  $d_{xy}(b_{1g})$  orbital.<sup>20</sup> The same result<sup>21</sup> is found for  $[\text{Cu}(\text{mnt})_2]^{2-}$ . The experimental data thus

(16) (a) Schläpfer, C. W.; Nakamoto, K. *Inorg. Chem.* **1975**, *14*, 1338. (b) Browall, K. W.; Interrante, L. *J. Coord. Chem.* **1973**, *3*, 27. (c) Siiman, O.; Fresco, J. *Inorg. Chem.* **1971**, *10*, 297.

(17) (a) Sartain, D.; Truter, M. R. *J. Chem. Soc., Chem. Commun.* **1966**, 382. (b) Sartain, D.; Truter, M. R. *J. Chem. Soc. A* **1967**, 1264.

(18) (a) Wing, R. M.; Schlupp, R. L. *Inorg. Chem.* **1970**, *9*, 471. (b) Ramakrishna, B. L.; Manoharan, P. T. *Inorg. Chem.* **1983**, *22*, 2113. (c) Kuppasami, P.; Mahadevan, C.; Seshasayee, M.; Manoharan, P. T., unpublished results.

(19) (a) Endres, H.; Keller, H. J.; Moroni, W.; Nöthe, D. *Acta Crystallogr., Sect. B* **1979**, *B35*, 353. (b) Eisenberg, R.; Ibers, J. A. *Inorg. Chem.* **1965**, *4*, 605. (c) Eisenberg, R.; Ibers, J. A.; Clark, R. J. H.; Gray, H. B. *J. Am. Chem. Soc.* **1964**, *86*, 113.

(20) (a) Geiger, Jr., W. E.; Allen, C. S.; Mines, T. S.; Senftleber, F. C. *Inorg. Chem.* **1977**, *16*, 2003. (b) Mines, T. E.; Geiger, W. E., Jr. *Inorg. Chem.* **1973**, *12*, 1189.

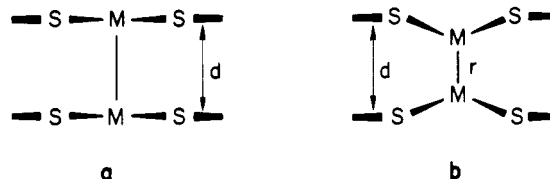
(21) Maki, A. H.; Edelstein, N.; Davidson, A.; Holm, R. *J. Am. Chem. Soc.* **1964**, *86*, 4580.

suggest that the  $d_{xy}$  orbital should be below  $2a_{1g}$ , and the inverted order in our diagram could be attributed either to our parameterization (a test calculation with an ionization potential of the sulfur 3p orbitals smaller by 2 eV changes the ordering of these levels without significantly affecting the rest of the diagram) or to the well-known overestimation of the  $\sigma$ -antibonding interactions by the extended Hückel method. However, the different experimental results for other  $d^9$  compounds ( $\text{Pt}^{\text{I}}$  and  $\text{Au}^{\text{I}}$ )<sup>20,22</sup> suggest that the differences between those levels are small and their relative positions may vary as the electronegativity of the metal atom is changed. On the other hand, the relative ordering of these orbitals is not relevant to the subsequent study. We shall proceed to use the MO diagram in Figure 1 as a reasonably good one for the latter transition metals.

## Dimers of Metal Bisdithiolenes

Let us try to understand how the transition-metal bisdithiolenes dimerize and why some metals form metal-sulfur while others form metal-metal bonded dimers.

A common characteristic of both kinds of dimers is the displacement of the metal atom out of the ligands' plane. There are two possible reasons for this distortion. First, the square-pyramidal stereochemistry might be more stable than one with the metal atom in the basal ligand plane. But this would apply only for  $d^8$  and possibly  $d^7$  pentacoordinated metals.<sup>23</sup> Second, the fifth ligand is in the present case a whole metal bisdithiolenes molecule, and as two planar molecules approach each other at a distance suitable for metal-metal or metal-sulfur bonding, the repulsion between the sulfur  $\pi$  lone pairs becomes very strong. If both ligand planes are kept at a reasonably large distance, say  $d$  in **12a** (a side projection of two metal bisdithiolenes molecules), a displacement of the metals out of the plane is necessary to bring the metal atoms to a bonding distance  $r$ , **12b**. This might happen even though



## 12

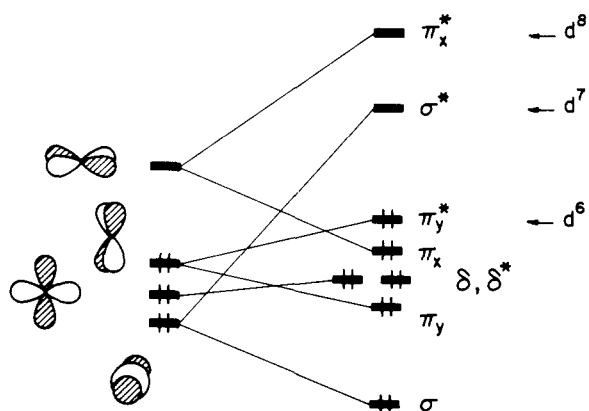
some weakening in the intramolecular M-S bond might result for  $d^6$  or lower electron counts. The repulsion of the  $\pi$  systems of both molecules is thus an important reason for the pyramidalization of the metal atoms in the dimers.

The stability of the dimers therefore depends on a delicate balance between three main factors: (a) the formation of new bonds between monomers, (b) the pyramidalization of the metal atom, and (c) the repulsion between the  $\pi$  electrons of both monomers.

Let us look first at the electronic structure of the metal-metal bonded dimers **2b** with the aid of an extended Hückel calculation on a model compound  $[\text{Pt}(\text{edt})_2]_2$  with a metal-metal distance of 3.03 Å and identical inter-ring separation. The interactions that appear (**13**) are the well-known  $\sigma$ ,  $\pi$ , and  $\delta$  ones present in every metal-metal bonded  $\text{M}_2\text{L}_8$  compound, except for a small yet significant difference: the  $\pi$  orbitals are not degenerate in this case and, consequently, the level sequence is altered as shown in **13**.  $\pi_x$  is not degenerate with  $\pi_y$ , nor  $\pi_x^*$  with  $\pi_y^*$ . The  $\pi$  bonding for the  $d^6$ -electron count is accomplished through the  $d_{xz}$  orbitals. It should be recalled that the  $d_{xz}$  has important contributions from sulfur  $p_z$  orbitals (MO  $2b_{3g}$  in Figure 1), and thus the metal-metal  $\pi$  bond has some ligand-ligand  $\sigma$  character. In any case, the existence of this bond should be sufficient to hinder the relative rotation of the two monomers, as experimentally found.<sup>5</sup>

(22) Schupp, R. L.; Maki, A. H. *Inorg. Chem.* **1974**, *13*, 44.

(23) Rossi, A. R.; Hoffmann, R. *Inorg. Chem.* **1975**, 1065.



13

If one believes the calculated  $\pi^*$  over  $\sigma^*$  order of the empty levels,<sup>24</sup> then the addition of one electron to the  $\sigma^*$  orbital ( $d^7$ ) should leave us with only a  $\pi$  M-M bond. An additional electron ( $d^8$ ) would finally destroy the M-M  $\pi$  bond too. The changes in metal-metal bond distances from 2.7–2.8 Å (Pd and Pt,  $d^6$ ) to 3.4 Å (Pt,  $d^7$ ) to 4.0 Å (Cu,  $d^8$ ) together with the fact that the  $d^7$  compound still shows an eclipsed conformation (for references, see Table I) seem to agree with the  $\pi^*$  over  $\sigma^*$  pattern.

None of the first-row transition metals with configurations  $d^5$  to  $d^7$  form this kind of dimer. We feel the inter-ring repulsion might be responsible for this observation, because the two rings should be closer for the smaller metals to be at a distance suitable for bonding. Thus, we next study two possible ways of reducing that repulsion. One, of course, is the slippage toward the metal-sulfur bonded dimer **2a** experimentally found. But we could also expect that a rotation of both rings around the metal-metal bond **14** could suffice to avoid such repulsions, as seems to be the case for metal bisdioximates.<sup>25,26</sup>

If we look at the variation upon rotation of the energy of two superimposed monomers **14** without the metal atom, at the distances associated with a first-row (2.8 Å) and second- or third-row (3.03 Å) transition metal, respectively, a minimum appears at  $\alpha = 45^\circ$ . The same minimum is found if one considers just the



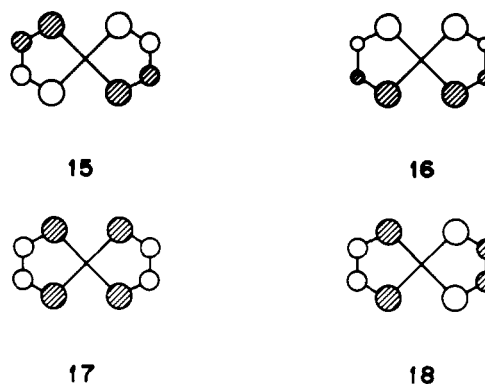
14

sulfur  $\pi$  lone-pair fragment molecular orbitals (FMO's) **15–18**, since they are responsible for the largest part of the inter-ring repulsion. However, substantial repulsion remains even for  $\alpha = 45^\circ$  because as some overlaps decrease, others are enhanced upon rotation (Figure 2). As an example, the overlap between the orbitals **16** of both fragments (and hence the repulsion) decreases from 0.148 to 0.041 upon rotation but is still smaller for the slipped arrangement **2a** (0.016). Similar results are obtained for the remaining overlaps between orbitals **15–18** of the two monomers, indicating that slippage provides a more efficient way to relieve repulsions than the rotation.

(24) At shorter Pt-Pt distances (2.7 Å), the  $\sigma$ - $\sigma^*$  splitting becomes large enough to change this order, but shorter distances appear only for the  $d^6$  complexes. In these molecules,  $\sigma^*$  and  $\pi^*$  orbitals are empty and their relative position is irrelevant as long as we are not interested in spectroscopic or photochemical properties.

(25) Endres, H.; Keller, H. J.; Lehmann, R.; Poveda, A.; Rupp, H. H.; van de Sand, H. Z. *Naturforsch., B* **1977**, *32B*, 516.

(26) Alvarez, S.; Canadell, E. *Solid State Commun.* **1984**, *50*, 141.



The bonding in the slipped dimers involves the  $d_{z^2}$  orbitals  $1a_g$  and a mixture of the ligand  $\pi$  lone pairs (i.e.,  $2b_{3g}$ ,  $1b_{3g}$ , and  $b_{1u}$  in Figure 1). For simplicity, we consider now the dimer as composed of two planar molecules; the intermolecular bonding does not change significantly upon pyramidalization, as checked with a calculation. The only existing element of symmetry in the dimer is an inversion center located at the center of the MSMS square. Consequently, important mixing of the different  $\pi$  orbitals occurs, and finally one is left with only the  $d_{z^2}$  orbital and the  $p_z$  orbital of the apical sulfur atom in each monomer to interact. The symmetry adapted combinations of both  $d_{z^2}$  orbitals are  $g$  and  $u$  (Figure 3); also the  $p_z$  orbitals can form a symmetric and anti-symmetric combination. Now, the combinations of the same symmetry can interact, giving rise to two bonding and two antibonding levels. For  $d^6$  compounds or lower electron counts, the low-lying empty  $d_{xz}$  orbitals can accommodate the electrons that were previously in  $d_{z^2}$ , while for  $d^8$  compounds the antibonding levels would be filled and the net interaction would be repulsive.

Two metal-sulfur bonds are formed for an electron count of  $d^6$  or lower, since for a lower number of electrons nonbonding  $d$  orbitals are emptied (cf. the structural data for  $d^5$  and  $d^6$  Co dimers in Table I). No bonding interaction exists for the  $d^8$  case: the shortest distance formed in a  $d^8$  "dimer" is Au-S = 3.96 Å. The  $d^7$  compounds are in between, forming only very weak bonds ( $\sim 3.5$  Å for Ni-S).

So far, we can explain quite well the bonding and structures for both kinds of dimers. We should then have enough information to understand why, for the same electron count ( $d^6$ ), the first-row transition metals form metal-sulfur bonds while Pd and Pt form metal-metal bonds. Let us try.

Conceptually, one can imagine that the total energy of a dimer contains three contributions: one consisting of metal-metal or metal-sulfur bonding, another being a ligand-ligand repulsion, and a third one being the pyramidalization of the metal atom.

Pyramidalization produces partial loss of the metal-ligand  $\pi$  bonding within the monomer and is thus a factor favoring the M-M dimerization mode. The out-of-plane displacements of both metal atoms contribute to a shortening in M-M distance without decreasing the inter-ring distance. However, this energy term is not large for small displacements, and it has probably little influence on the choice between the two available dimerization modes. As an illustration of the importance of this effect, the calculations show a small change in the average intramolecular Ni-S overlap populations in a  $[\text{Ni}(\text{edt})_2]_2$  dimer with M-S bonds for a displacement of 0.3 Å (from 0.541 to 0.514). The main role of pyramidalization is therefore to allow short M-M or M-S distances while simultaneously avoiding large inter-ring repulsions.

Schematic energy curves showing the contributions of the two remaining components and a composite total energy curve can then be drawn (Figure 4). For the metal over the metal configuration in Pt, the inter-ring distance at the M-M bond length is large enough to keep the repulsive term (labeled S-S) to a small value and the total energy (dashed line) is controlled by the M-M interaction. In the metal over sulfur configuration, the minimum in the energy curve of the M-S interaction corresponding to a bonding distance appears at smaller values of  $d$ , where the repulsion is important, even though a large part of the previous

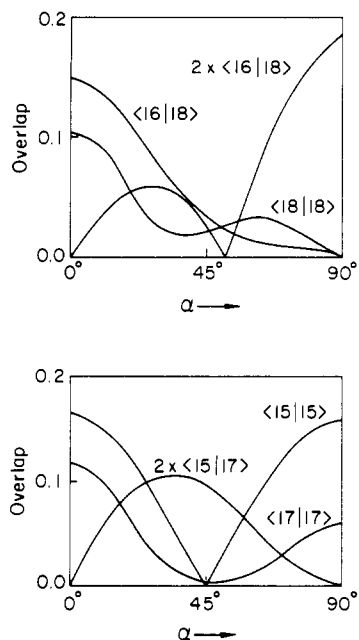


**Figure 2.** Absolute value of the overlap integrals of the  $\pi$  orbitals of two  $S_4C_4H_4$  units at different rotation angles.

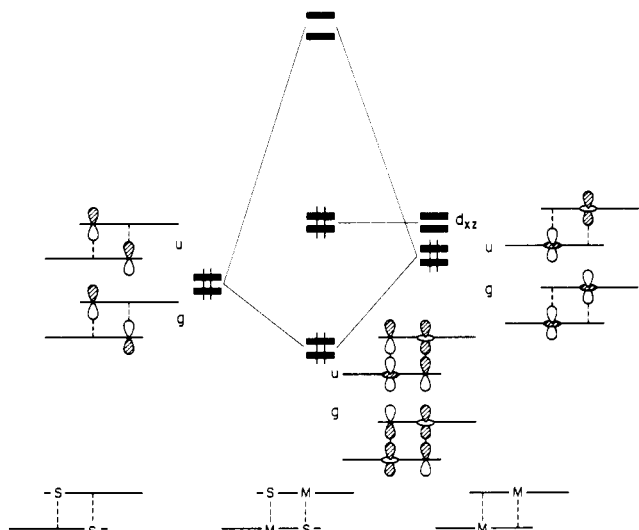


**Figure 3.** Interaction diagram for the square  $M_2S_2$  unit in the M-S bonded dimer  $[Ni(S_2C_2H_2)_2]$ .

repulsion is avoided in this conformation. The total energy should then show a shallower minimum, or no minimum at all, as represented in Figure 4.

For first-row transition metals, not only the bonding distances are smaller, but also the R groups in **1** (CN,  $CF_3$ , benzo, and  $COOCH_3$ ) are bulkier than for Pd and Pt (where R = H). This results in a more drastic variation in the ligand-ligand repulsion curve. As a consequence, the situation is reversed from the Pt case: a minimum should appear for the M-S dimer but not for the M-M dimer.

These qualitative arguments are in fact supported by detailed calculations for Ni and Pt dimers.<sup>27</sup> The choice between the two

(27) In the actual computed curves for dimerization, there appear small discontinuities, ultimately leading to small activation energies. These discontinuities are the result of level crossings. That such crossings should occur is clear from diagram 13—the dimerization of a low-spin  $d^6$  monomer is a “forbidden” reaction. The activation energies found are very small because the levels involved in the crossing ( $d_{xz}$  and  $d_{yz}$ ) are very close in energy. A similar explanation of the easing of a forbidden reaction may apply to the formation of adducts of olefins with  $Ni(mnt)_2$ : (a) Schrauzer, G. N.; Ho, R. K. Y.; Murillo, R. P. *J. Am. Chem. Soc.* **1970**, *92*, 3508. (b) Wing, R. M.; Tutsin, G. C.; Okamura, W. H. *J. Am. Chem. Soc.* **1970**, *92*, 1935–1939. (c) Baker, J. R.; Hermann, J. R.; Wing, R. M. *J. Am. Chem. Soc.* **1971**, *93*, 6486–6489.

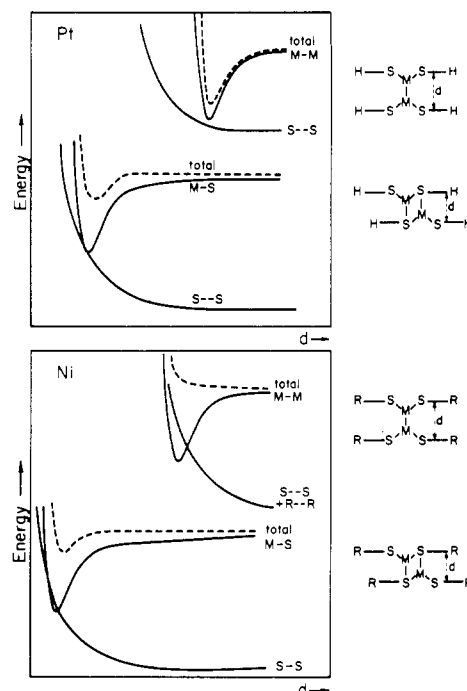


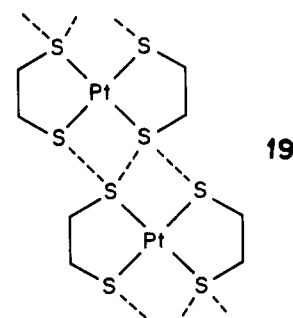
**Figure 4.** Schematic potential energy curves for M-M and M-S dimerization of  $[M(S_2C_2H_2)_2]$ ; M = Pt (above) and Ni (below). The solid lines represent the bond formation and lone-pair repulsion, respectively, and the dashed line the resulting total energy.

alternative dimeric structures seems to rely on a delicate balance between the intervening forces. The reported dimeric compounds (Table I) clearly represent the two extreme cases: first-row metals and bulky substituents form M-S dimers whereas larger metals with small substituents form M-M dimers. What would happen in the intermediate cases is not easy to predict, but it might well be that appropriate changes in the substituents could allow the preparation of M-M dimers of first-row transition metals or M-S dimers of heavy metals.

### One- and Two-Dimensional Stacks

If a regular chain is to be formed, the out-of-plane distortion of the metal is no longer available. Only planar bisdithiolenes are compatible with such a chain, and assuming a metal over metal stacking, we would not expect metal-metal distances shorter than  $\sim 3.1$  Å. At this separation, we have found that sulfur-sulfur repulsions become too large.

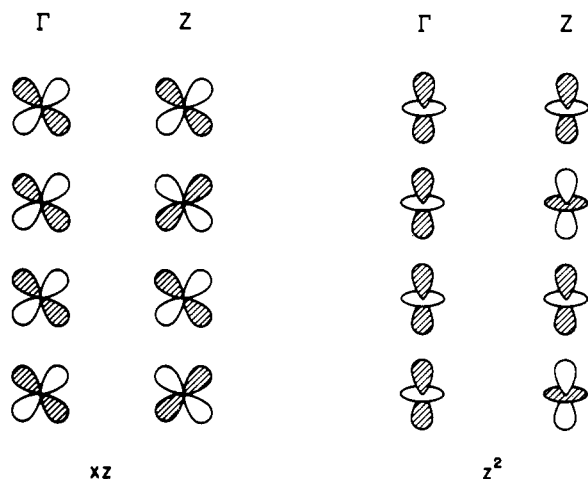
It has been pointed out by Kobayashi et al. that there are short contacts between the sulfur atoms in parallel stacks as in **19** ( $S \cdots S \approx 3.5$ – $3.7$  Å),<sup>6a,c,d</sup> the two molecules represented lying in different planes. The same type of inter-stack contacts exist in the low-



pressure superconducting organic metal  $(TMTSF)_2ClO_4$  and other salts of  $TMTSF$ <sup>28,29</sup> ( $TMTSF$  = tetramethyltetraselenafulvalene)

(28) Bechgaard, K.; Carneiro, K.; Rasmussen, F. B.; Olsen, M.; Rindorf, G.; Jacobsen, C. S.; Pedersen, H. J.; Scott, J. C. *J. Am. Chem. Soc.* **1981**, *103*, 2440.

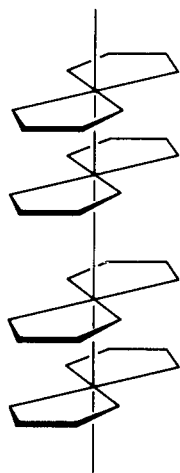




## 22

$d^8$  polymers are not likely to form—the explanation that emerges from the band structure is essentially the same as we constructed for the dimers. Both the  $d_{xz}$  and  $d_{z^2}$  bands are filled for  $d^8$ . The antibonding levels in the upper (antibonding) part of each band are more destabilized with respect to the monomer than their lower (bonding) part is stabilized. Forming a stack is thus energetically unfavorable. Also, the large dispersion shown by the occupied  $\pi$  lone-pair bands, mentioned above, indicates large inter-ring repulsion.

With one electron less,  $d^7$  systems would be predicted to be metallic according to Figure 5. But it is well-known that such systems are unstable toward a pairing distortion.<sup>30</sup> It is easiest to examine the workings of such a distortion on a one-dimensional model chain, **23**, where one M–M bond is short and another long.



## 23

The computed band structure is in Figure 6. As the unit cell of our chain consists now of two molecules, eight d bands appear (if you can find only seven in Figure 6, it is not your fault: the two  $d_{x^2-y^2}$  bands have the same energy and appear superimposed in the diagram). A gap is introduced,<sup>31</sup> and the system is stabilized by the pairing distortion. It is semiconducting, the experimental room-temperature conductivity<sup>6a</sup> being  $2.5 \times 10^{-5} \Omega^{-1} \text{cm}^{-1}$ .

What happens with one less electron ( $d^6$ )? The calculated Pt–Pt overlap population between nearest neighbors increases from 0.010 ( $d^7$ ) to 0.030 ( $d^6$ ). This fact can be understood in part from Figures 5 and 6 since the electron is taken away from the upper (antibonding) part of the  $z^2$  band (Figure 5) or, in a distorted chain, from the  $z^2$  band, which is the antibonding counterpart of the lower bonding  $z^2$  (Figure 6).

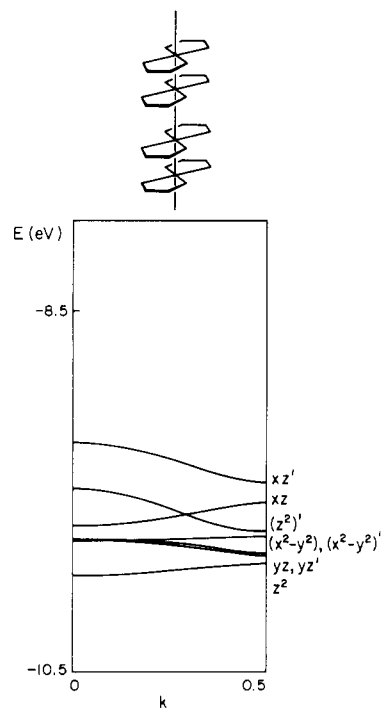


Figure 6. d bands for a Peierls-distorted stack of  $\text{Pt}(\text{edt})_2$ .

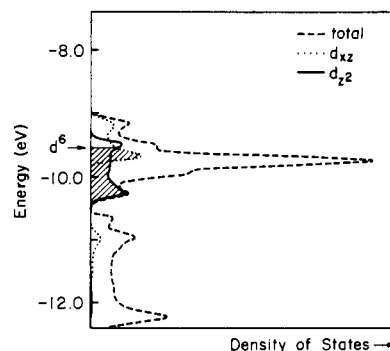
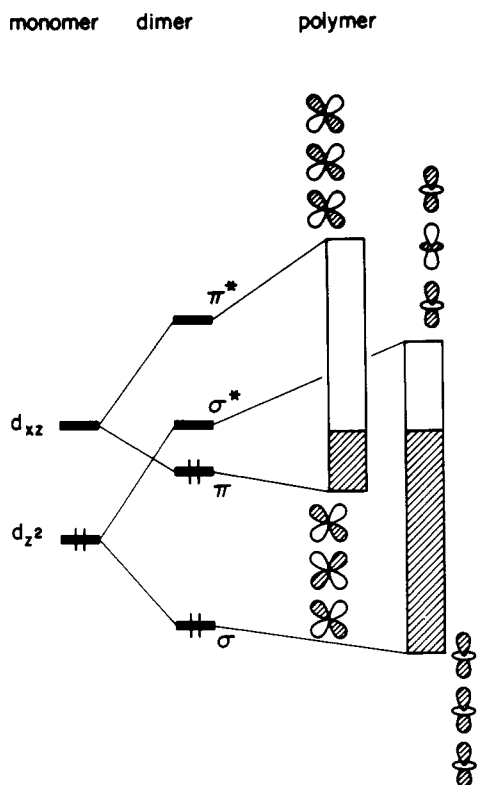


Figure 7. Density of states of a  $\text{Pt}(\text{edt})_2$  stack (dashed line) and contribution of  $d_{xz}$  (dotted line) and  $d_{z^2}$  (solid line) orbitals.

One might expect a decrease in bond lengths in the chain and perhaps some distortion. However, what is experimentally found is not a chain but a dimer.<sup>5</sup> The average energy per monomer calculated for the chain is 1.4 eV higher than that in a dimer, at the same distance and with a planar conformation in the monomers. This is in agreement with the experimental findings. However, we know that we cannot trust total energies calculated by the extended Hückel method, and so we look for a sound qualitative argument behind the result.

Let us look at the density of states (DOS) in the one-dimensional chain and at the  $xz$  and  $z^2$  components of the DOS (Figure 7). The dashed line represents the total density of states and shows a peak at about  $-10$  eV corresponding to the d bands of Figure 6. The contribution of the  $d_{z^2}$  orbitals is represented by the solid line and that of the  $d_{xz}$  orbitals by a dotted line; the shaded part is that filled for a  $d^6$  compound. What the diagram shows is that a large part of the upper  $d_{z^2}$  band is filled, leaving only a weak  $\pi$  bond between monomers in the chain. The same conclusion is shown in a schematic way in **24**. That structure also reminds us of the dimer levels. In the  $d^6$  dimer, there is a  $\sigma$  bond and a  $\pi$  bond. In the polymer the antibonding part of the  $\sigma$  band starts to fill before all the bonding part of the  $\pi$  band is occupied. This is the reason the dimer is preferred.

We will not attempt to discuss in detail the cases with noninteger oxidation states, but it is clear that the energy difference between the distorted and undistorted chains should be smaller and the latter may be found at room temperature. If that happens, the

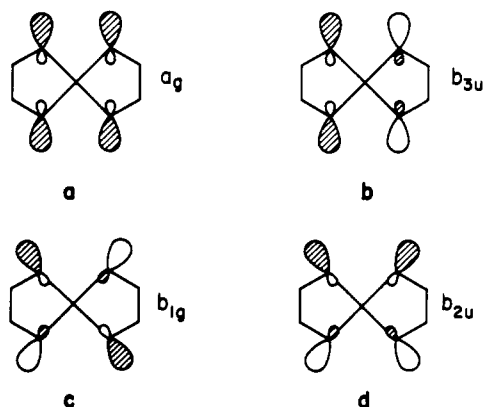


24

diagram of Figure 6 applies and the partially occupied  $d_{xz}$  band (calculated bandwidth = 0.35 eV, the estimated bandwidth from infrared reflectivity measurements is 0.3–0.4 eV<sup>6b</sup>), is responsible for the conductivity.

### Inter-stack Interactions

For the lateral interactions between stacks, we will focus on the two sets of sulfur lone-pair bands,  $\sigma$  and  $\pi$ . Those interactions are reflected at the right-hand side ( $\Gamma Y$  line) of the band diagram (Figure 5). The  $\sigma$ -type lone pairs are best oriented to interact amongst themselves and should produce substantial dispersion. That no band appears to be wide along the  $\Gamma Y$  line is in some sense an accident of symmetry. The orbitals from which these bands are built up (**25**) are all symmetric with respect to reflection on the  $xy$  plane. Two of them ( $a_g$  and  $b_{2u}$ ) are symmetric and two



25

are antisymmetric ( $b_{3u}$  and  $b_{1g}$ ) with respect to reflection on the  $yz$  plane. Hence, crossing is forbidden, and the bands appear as if they were narrow even though the interaction is important. This is best seen in the composition of the bands at both the  $\Gamma$  and the  $Y$  points. For instance, the  $a_g$  orbital **25a** provides the main

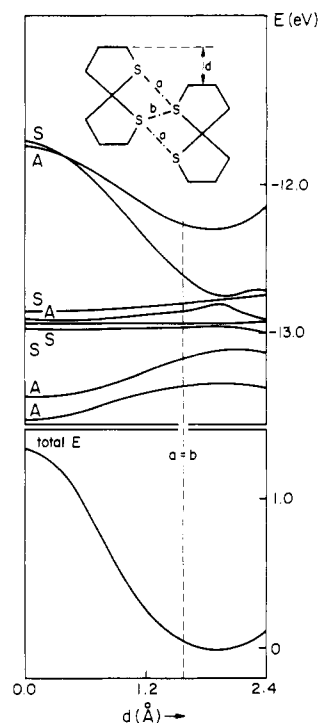


**Figure 8.** Walsh diagram (above) and total energy curve (below) for the sliding of two neighboring  $\text{Pt}(\text{edt})_2$  molecules. The two higher and two lower lines in the Walsh diagram correspond to the sulfur  $\sigma$  lone pairs, while the intermediate four correspond to the  $\pi$  lone pairs.

**Table II.** S...S Inter-stack Contacts

|   | Pt(edt) <sub>2</sub><br>calcd | ref 6c | M(dithiolenes) <sub>2</sub> <sup>2-</sup><br>ref 6d | ref 6g      |
|---|-------------------------------|--------|---|-------------|
| a | 3.68                          | 3.75   | 3.74  | 3.66 av     |
| b | 3.49                          | 3.55   | 3.65  | 3.52 values |

contribution to the lowest of these bands at  $\Gamma$  point but appears as the major component of the highest  $\sigma$  lone-pair band at the  $Y$  point, after two avoided crossings. In a similar way, the orbitals  $b_{3u}$ ,  $b_{1g}$ , and  $b_{2u}$  (**25b–d**) appear in different bands at both extremes of the  $\Gamma Y$  line, indicating avoided crossings.

A similar situation is found for the  $\pi$  lone-pair bands along the  $Z\Gamma$  line. The symmetry point group along this line is  $C_{2v}$ ; each of the sulfur  $\pi$  orbitals (**15–18** with some  $d$  admixture) belongs to a different symmetry representation, and the interaction is apparent now in the large bandwidths. Only avoided crossings with the  $\sigma$  lone pairs are operative in this case.

As in both cases that the large interactions take place between filled orbitals, they are repulsive. The ideal packing assumed so far must be changed in order to decrease these repulsions. A strategy may be constructed by noting that the two sources of repulsive interaction are potentially separable. The  $\sigma$  lone-pair repulsions depend essentially on the relative positions of neighboring stacks while the  $\pi$  lone-pair repulsive depends mainly on the stacking pattern.

For a fixed inter-stack distance, an obvious way to reduce the S...S repulsions is the lateral sliding **21**  $\rightarrow$  **19**. This motion has been studied with calculations on two  $\text{Pt}(\text{edt})_2$  molecules placed side by side at different relative positions along the  $x$  axis; the total energy (Figure 8, bottom) reaches a minimum past the point in which a sulfur atom in one of the  $\text{Pt}(\text{edt})_2$  molecules is equidistant from two sulfur atoms in the neighboring one (i.e.,  $a > b$  in Figure 8), in excellent agreement with the experimental structures of platinum dithiolenes stacks<sup>6c,d</sup> and of  $\text{Ni}(\text{dmit})_2$  stacks<sup>6f,g</sup> (Table II).

A portion of the Walsh diagram including only the  $\sigma$  lone pairs (Figure 8, top) shows that the minimum in the energy curve corresponds to a minimum in their splittings. It is also evident from the Walsh diagram that these splittings are still sizeable and

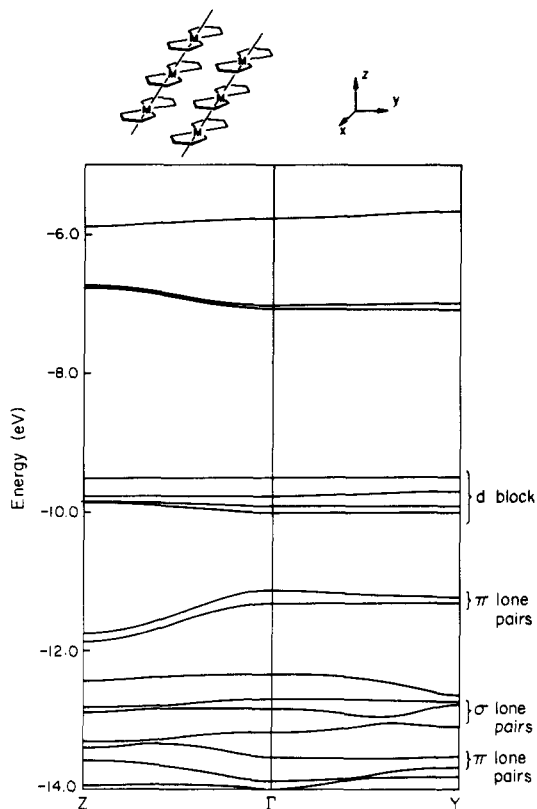
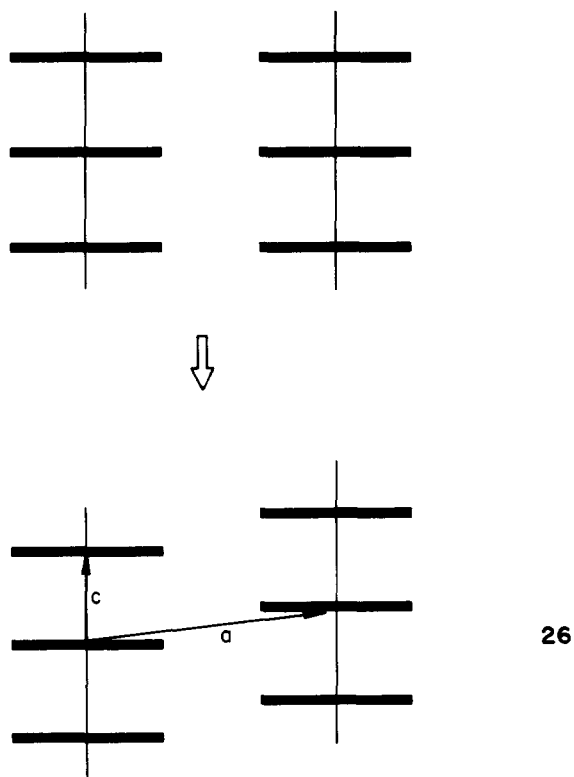
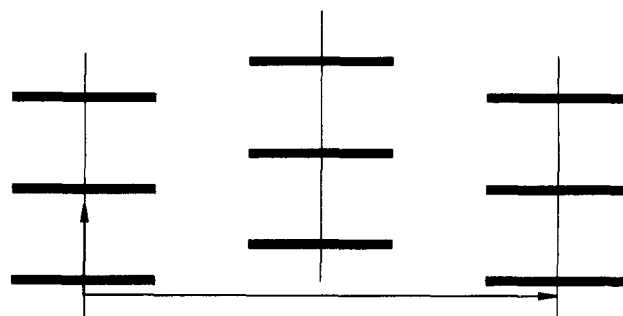


**Figure 9.** Band structure of Pt(edt)<sub>2</sub> after sliding and vertical displacement of neighboring stacks and intra-stack slipping.

so are the repulsions. Now, a vertical displacement of the neighboring stacks, **26**, can eliminate the rest of the repulsion;

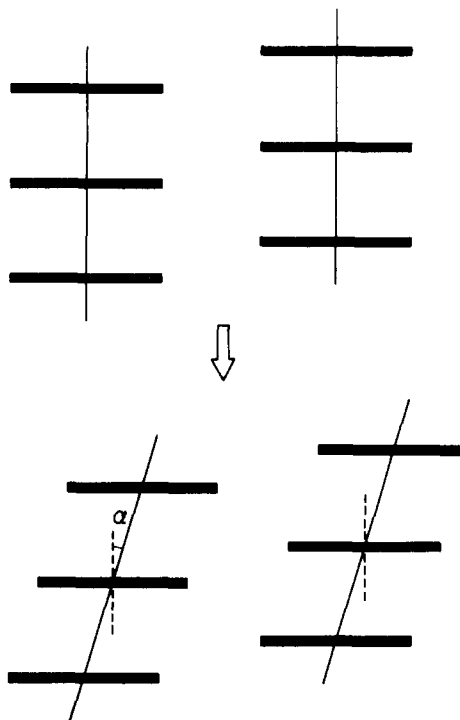


a tight binding calculation on this two-dimensional system gives a minimum for a displacement of half the inter-ring distance. This displacement would take the unit cell from monoclinic to triclinic, as found in a number of systems.<sup>2e,6a,c,d,f</sup> A monoclinic system is still available if the unit cell is larger as in **27**.<sup>6g</sup>



**27**

After these changes in the crystal arrangement of the stacks, the band structure (not shown here) indicates that the repulsion along the  $\Gamma Y$  line has almost disappeared. Let us now look at the intra-stack interactions. If only interaction between the partially filled HOMO's were considered,<sup>32</sup> we would conclude that the eclipsed stacking is the most stable. However, we have seen that important destabilization arises from the interactions of the four  $\pi$  lone-pair orbitals. Therefore, a slipping from the eclipsed stacking should produce a decrease in the repulsion between these orbitals (essentially **25**). At the same time the  $d_{z^2}$  and  $d_{xz}$  (the latter containing an important contribution of a ligand  $\pi$  orbital) interactions act in the opposite direction. As a result, a minimum in the average energy per unit cell for the slipping **28** is calculated at  $\alpha \approx 30^\circ$ . In two reported structures, angles



**28**

of  $78^\circ$ <sup>6g</sup> and  $33^\circ$ <sup>6f</sup> have been found; in other cases the slipping angle is not reported but the existence of slippage is obvious.<sup>6a,c,d</sup> A similar slippage is apparent, along either the  $x$  or  $y$  axis, in tetrathiofulvalene and tetraselenafulvalene salts and their derivatives.<sup>33-35</sup> It can be anticipated that bulkiness of the R group in the ligand as well as a poor metal-metal interaction might produce large slipping angles.

If the band structure is computed again with a new packing pattern which incorporates the rearrangements discussed so far (**21**  $\rightarrow$  **19**, **26**, and **27**), the diagram presented in Figure 9 is obtained. Note how the bandwidths of the lower occupied bands ( $\sigma$  and  $\pi$  lone pairs) have been largely decreased from those in Figure 5. On the other hand, as a result of the slipping, dispersion

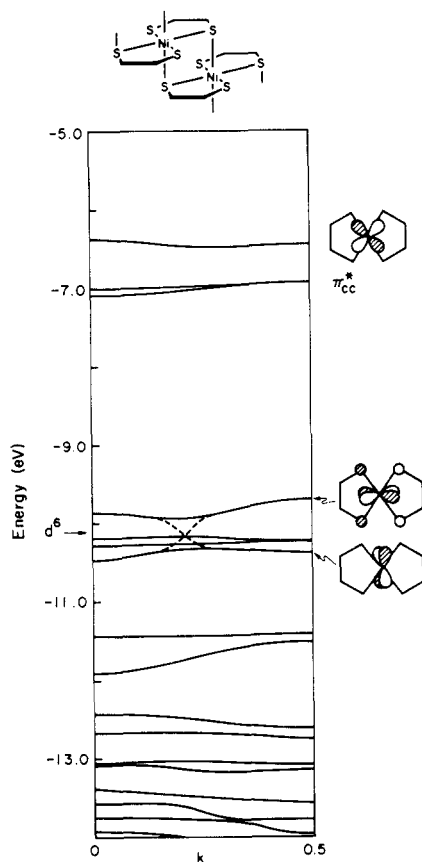
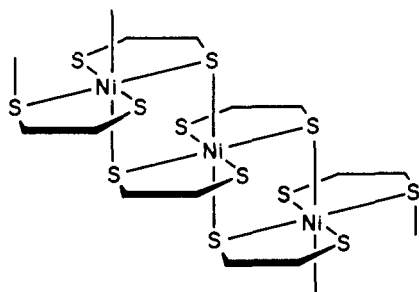


Figure 10. Band structure for a sulfur-over-metal stacking of Ni(edt)<sub>2</sub> molecules.

appears for the  $\pi$  lone-pair bands along the  $\Gamma Y$  line and the mixing of  $d_{xz}$  with 17 should also produce dispersion for the corresponding band. The fact that this band appears quite narrow in Figure 9 is undoubtedly due to the insufficient amount of mixing produced by our parameterization. This would account for the two-dimensional conductivity found by Valade et al.<sup>6f</sup> for (NBu<sub>4</sub>)<sub>0.29</sub>[Ni(dmit)<sub>2</sub>] as well as for the relatively high conductivity of Li<sub>0.5</sub>[Pt(mnt)<sub>2</sub>] $\cdot$ 2H<sub>2</sub>O found by Kobayashi et al.<sup>6c</sup> despite the severe pairing distortion observed (see Table I).

Is a metal-sulfur-bonded stack possible? Although we have shown before that important pyramidalization is needed to form a similar dimer, especially for first-row transition metals, we cannot rule out the existence of such chains with heavier metal atoms. We computed the band structure for a hypothetical Ni(edt)<sub>2</sub> stack with a separation of 3.2 Å, 29. Figure 10 shows a band gap for



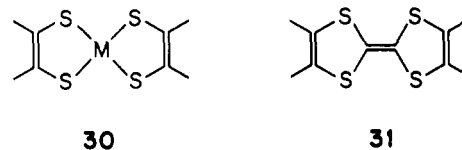
29

$d^6$  compounds due to an avoided crossing caused by the low symmetry of this arrangement. This is different from the metal-over-metal stacking pattern. As the higher d band (the unfilled conduction band for  $d^6$ ) contains mainly antibonding intercell crystal orbitals both at the center and the edges of the Brillouin zone, it is clear that a net bonding situation between neighboring

unit cells would arise for  $d^2$  to  $d^6$  configurations. It is interesting to note that several related structures exist for bis(oxalato)cuprates.<sup>36</sup>

### An Isolobal Analogy for Extended Systems

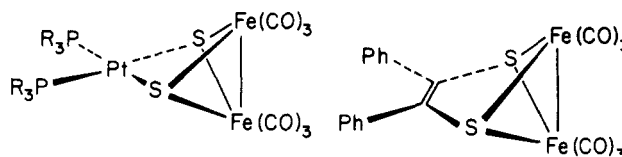
We have briefly mentioned some analogies between the metal bisdithiolene, 30, and tetrathiofulvalene, 31, stacks. We would like to show here how to extend that analogy to many other systems and, in particular, to extended systems. There exist for



30

31

instance some sulfido complexes<sup>37</sup> of type 32. There also exist dithiolene complexes 33.<sup>12c</sup> It is appealing to make an analogy

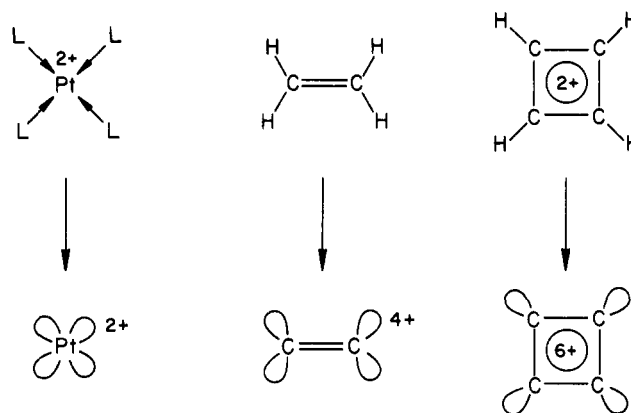


32

33

between the Pt and C<sub>2</sub> units. To be more precise, we will compare C<sub>2</sub><sup>4+</sup> and Pt<sup>2+</sup> and add, for reasons to be made clearer later, a square-planar C<sub>4</sub><sup>6+</sup> unit.

Consider a  $d^8$  PtL<sub>4</sub> complex and an ethylene and a cyclobutadienyl dication. Next remove from these, as indicated in 34, four ligands with their electron pairs. For the organic molecules this means removing H as H<sup>-</sup>. Since a localized covalent or dative



34

bonding picture was not a bad one for either the organic or the inorganic molecules in the first place, what remains behind when the hydrides or ligands leave is a set of four hybrids pointing toward the missing ligands. These acceptor orbitals transform as  $A_g + B_{1g} + B_{2u} + B_{3u}$  in  $D_{2h}$  and are shown in Figure 11. Various identifications may be made: the metal's  $s(a_g)$  orbital is related to the nonbonding combination of the sp hybrids in C<sub>2</sub>; the  $d_{x^2-y^2}(b_{1g})$  orbital finds its analogue in  $\pi^*_y$  of C<sub>2</sub>; the metal  $p_y(b_{2u})$  correlates with  $\pi_y$  of C<sub>2</sub> and its  $p_x(b_{3u})$  with  $\sigma_s^*$  of C<sub>2</sub>. A similar correlation can be found with the orbitals of the C<sub>4</sub> fragment. These three fragments are thus isolobal,<sup>38</sup> 35, provided



35

reactions in which carbon-carbon  $\sigma$  bonds are broken are not considered.

This isolobal analogy should allow one to find interesting correlations between two highly developed areas of chemistry: the organic alkenes and the  $d^8$  square-planar transition-metal com-

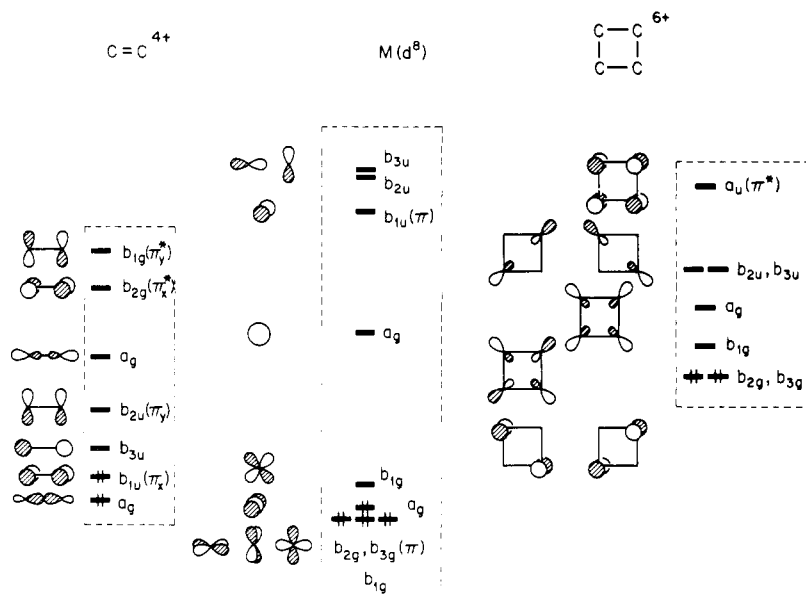
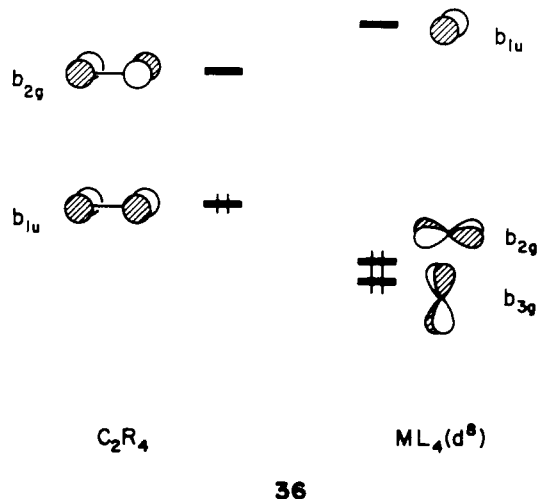


**Figure 11.** Valence orbitals of the isolobal fragments  $C_2^{4+}$ ,  $M(d^8)$ , and  $C_4^{6+}$  perturbed by a rectangular array of hydride ligands at a long distance.

plexes. It will also prove useful in the design of extended one- and two-dimensional structures. A similar analysis shows that  $C\equiv C^{2+}$  is isolobal with  $M(d^{10})$  and  $C-C^{6+}$  with  $M(d^6)$ .

The  $\pi$  orbitals of these systems deserve more careful consideration. Once four ligands are attached to the central cores, the four empty  $\sigma$  orbitals are pushed up in energy and one is left with only the  $\pi$  orbitals, **36**, in the valence zone, as well as  $d_{xy}$  in the



metal which is nonbonding and is omitted for simplicity. The  $\pi$  orbitals of the  $C_2$  fragment find their analogues on the metal side, except that they are inverted in energy order. This inversion is something already present in other isolobal analogies.<sup>38</sup>

Now we can look back at the stacking properties of metal bisdithiolenes and tetrathiofulvalenes. In the same way that dithiolenes show very weak interaction for  $d^8$  metals and stronger interactions for  $d^7$  and  $d^6$ , leading to dimer formation (Table I), the neutral TTF molecules stack with larger separation than the cationic compounds,<sup>39</sup> which tend to dimerize. On the other hand, regular chains are formed for nonintegral oxidation states in both cases. Also for TTF derivatives, the integer oxidation states lead to poor electrical conductivity, but noninteger ones are good conductors, as found for dithiolenes. A look at **36** suggests that TTF and  $M(edt)_2$  can interact with each other, as found experimentally,<sup>40</sup> forming even solid solutions in which TTF and  $Ni(edt)_2$  are randomly distributed along the stack.<sup>41</sup>

(40) (a) Kasper, J. S.; Interrante, L. V. *Acta Crystallogr., Sect. B* **1976**, *B32*, 2914. (b) Kasper, J. S.; Moncton, D. E. *Phys. Rev. B* **1979**, *B20*, 2341.

Finally, avoidance of inter-ring repulsions is at work in TTF too, causing rotation<sup>39e,42</sup> or slippage in the stacks.<sup>35,39e,g,h,i,40a</sup> Although the large interest exhibited by the community in the structural and electrical properties of TTF compounds justifies a deeper theoretical study, a rough picture should be contained in **36** and the previous discussion on metal bisdithiolenes.

### $C_2S_4$ , Ethylenetetrathiolate, Ligand

If we want to study the extended systems that the anionic forms of the ligands  $C_2S_4^{2-}$  and  $C_2S_4^{4-}$  might form (**6–9**), the most reasonable approach is to first explain the electronic structure of the ligand itself and how it interacts with metal fragments to form discrete compounds and then move to the study of the extended systems.

The dianionic form of ethylenetetrathiolate (ett) (**3**), is prepared by electrochemical reduction of  $CS_2$ ; the structure of a tetraalkylammonium salt has been reported.<sup>43,44</sup> Several complexes have recently been obtained in which the  $C_2S_4$  ligand is formed through coupling of two  $CS_2$  molecules, and their structures were determined. The coupling of two  $CSe_2$  molecules in a binuclear complex has also been reported.<sup>45c</sup> Complexes with the  $C_2S_4$  ligand can also be generated from 1,3,4,6-tetrathio-pentalene-2,5-dione.<sup>45f</sup> In most of them, ett presents a dithiolene-like coordination mode, **37**.<sup>12a,45</sup>

A tetranuclear compound **38** features dithiocarbamate-like coordination.<sup>12a</sup> And in a single remarkable example, that of

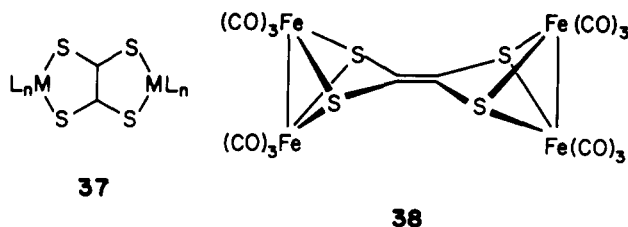
(41) (a) Interrante, L. V.; Browall, K. W.; Hart, H. R.; Jacobs, I. S.; Watkins, G. D.; Wee, S. H. *J. Am. Chem. Soc.* **1975**, *97*, 889. (b) Interrante, L. V.; Kasper, J. S. *AIP Conf. Proc.* **1979**, *53*, 205. For mixed stacks of transition-metal dithiolenes with other organic molecules, see ref 11, 9a, and 11. See also: Kisch, H.; Fernández, A. *Z. Naturforsch., B* **1985**, *40B*, 292 and references therein.

(42) Kasper, J. S.; Interrante, L. V.; Secaur, C. A. *J. Am. Chem. Soc.* **1975**, *97*, 890.

(43) A detailed discussion of the synthesis and head-to-head coupling mechanism of  $CS_2$  is given by: Hoyer, E. *Comments Inorg. Chem.* **1983**, *2*, 261. For the structure of  $(Ph_4P)_2C_2S_4$ , see ref 44a.

(44) (a) Lund, H.; Hoyer, E.; Hazell, R. G. *Acta Chem. Scand., Ser. B* **1982**, *B36*, 207. (b) Steimecke, G.; Sieler, H.-J.; Kirmse, R.; Hoyer, E. *Phosphorus Sulfur* **1979**, *7*, 49. (c) Jeroschewski, P. *Z. Chem.* **1981**, *21*, 412.

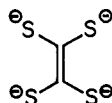
(45) (a) Maj, J. J.; Rae, A. D.; Dahl, L. F. *J. Am. Chem. Soc.* **1982**, *104*, 4278. (b) Englert, M. H.; Maj, J. J.; Rae, A. D.; Jordan, K. T.; Harris, H. A.; Dahl, L. F. "Abstracts of Papers", 187th National Meeting of the American Chemical Society, St. Louis, MO, April 1984; American Chemical Society: Washington, DC, 1984; INOR 280. (c) Bianchini, C.; Mealli, C.; Meli, A.; Sabat, M. *Inorg. Chem.* **1984**, *23*, 4125. (d) Harris, H. A.; Dahl, L. F., private communication. (e) Bianchini, C.; Mealli, C.; Meli, A.; Sabat, M. *J. Chem. Soc., Chem. Commun.* **1984**, 1647. (f) Vicente, R.; Ribas, J.; Solans, X.; Font-Altaba, M. unpublished results.



(Cp<sub>2</sub>Ti)<sub>2</sub>C<sub>2</sub>S<sub>4</sub>, dithiolene, and dithiocarbamate isomers coexist, in fact in one and the same crystal structure.<sup>45d</sup> Some compounds with an alkylated ett ligand are also well-characterized.<sup>46</sup>

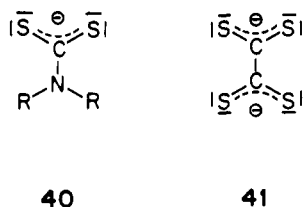
Finally, a number of polynuclear tetrathiolenes are known,<sup>47</sup> although no structure determination has been reported so far. These complexes present interesting conducting properties to be discussed later in more detail.

Although the tetraanion is not known by itself, the ett can be considered that way for electron-counting purposes when it is coordinated to a metal. Counting electrons in this fashion, **39**,



has the advantage that it allows comparisons with 1,2-dithiolenes, R<sub>2</sub>C<sub>2</sub>S<sub>2</sub><sup>2-</sup>, ett being just a "double dithiolene". We will consistently use the same electron-counting scheme for ett complexes throughout this paper (i.e., as C<sub>2</sub>S<sub>4</sub><sup>4-</sup>) regardless of its coordination mode, even though we might like to compare that ligand with dithiocarbamates, xanthate, trithiocarbonate, and similar ligands which are best described as monoanionic.

Let us be a little more explicit about this problem. A dithiocarbamate ligand, **40** a workhorse of modern inorganic chemistry, has four σ lone pairs on S and four π electrons. A "dithiocarbamate-like" formulation of ett is **41**, dianionic. It differs from



the tetraanionic **39**, in that the latter has 10 π electrons, the former eight. We will use **39**, C<sub>2</sub>S<sub>4</sub><sup>4-</sup>, even when the coordination mode resembles that of a dithiocarbamate ligand. Therefore, special caution must be taken when dealing with comparisons of the dithiocarbamate-like coordination mode of ett and real dithiocarbamates, since the oxidation state of the metal will not be defined in the same way in both cases.

The molecular orbital diagram of C<sub>2</sub>S<sub>4</sub><sup>2-</sup> can be obtained from the interaction of the orbitals of two CS<sub>2</sub><sup>-</sup> groups, in imitation of its real-life synthesis (Figure 12). The MO's are essentially the symmetric and antisymmetric combinations of the orbitals of bent CS<sub>2</sub> previously described.<sup>48</sup> The a<sub>1</sub> orbital is an empty π\* in the linear CS<sub>2</sub> molecule, which becomes semioccupied upon

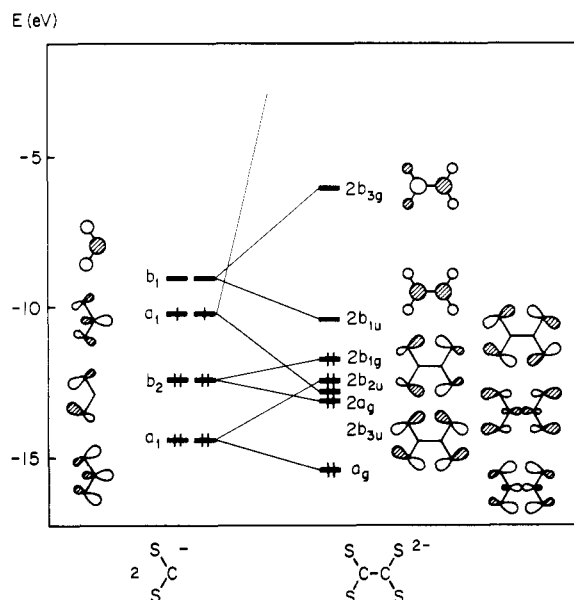


Figure 12. Interaction diagram for two CS<sub>2</sub><sup>-</sup> anions coupled head-to-head.

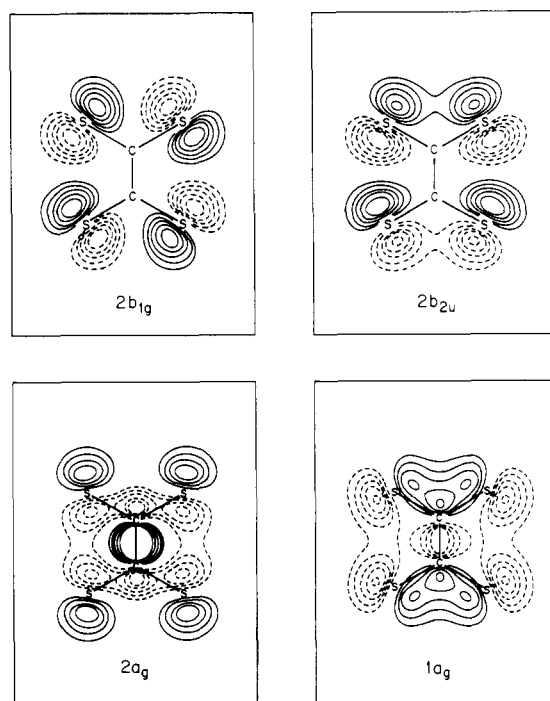
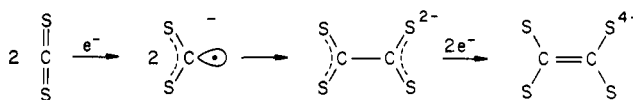


Figure 13. Contour maps for some σ lone-pair orbitals of C<sub>2</sub>S<sub>4</sub>.

reduction. This orbital is hybridized when the molecule is bent, as in **42**.



#### 42

It then presents a nice unpaired electron well positioned to form a carbon-carbon bond with another CS<sub>2</sub><sup>-</sup> unit, giving the dianionic ligand. This picture is in agreement with the single bond carbon-carbon distance (Table III) and the nonplanar structure of ett<sup>2-</sup>. In the tetraanionic ligand, on the other hand, the 2b<sub>1u</sub> orbital is filled (Figure 12), forming a localized carbon-carbon double bond. Looking at the carbon-carbon bond distances in coordinated

(46) (a) Cetinkaya, B.; Hitchcock, P. B.; Lappert, M. F.; Pye, P. L. *J. Chem. Soc., Chem. Commun.* **1975**, 683. (b) Cetinkaya, B.; Hitchcock, P. B.; Lappert, M. F.; Pye, P. L.; Shaw, D. B. *J. Chem. Soc., Dalton Trans.* **1979**, 434. (c) Lappert, M. F.; Shaw, D. B.; McLaughlin, G. M. *J. Chem. Soc., Dalton Trans.* **1979**, 427.

(47) (a) Poleschner, H.; John, W.; Kempe, G.; Hoyer, E.; Fanghänel, E. *Z. Chem.* **1978**, *18*, 345. (b) Poleschner, H.; Fanghänel, E.; Mehner, H. *J. Prakt. Chem.* **1981**, *323*, 919. (c) Poleschner, H.; John, W.; Hoppe, F.; Fanghänel, E. *J. Prakt. Chem.* **1983**, *325*, 957. (d) Ribas, J.; Vicente, R. *An. Quim.*, in press.

(48) Mealli, C.; Hoffmann, R.; Stockis, A. *Inorg. Chem.* **1984**, *23*, 56.

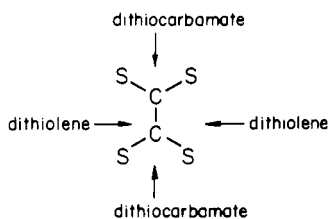
**Table III.** Selected Structural Data for ett Complexes<sup>a</sup>

| compd  | no. of d electrons <sup>b</sup> | bond dist |       | SCS ang | SCCS torsion ang | ref |
|--|---------------------------------|-----------|-------|---------|------------------|-----|
|  |                                 | C-C       | C-S   |         |                  |     |
| A. ett <sup>2-</sup>   |                                 | 1.461     | 1.70  | 129°    | 80°              | 44a |
| B. (ett)Fe <sub>2</sub> Cp' <sub>2</sub> L <sub>2</sub>                              | 5                               | 1.429     |       |         |                  | 45b |
| C. (ettMe <sub>4</sub> )CrL <sub>4</sub>   | 6                               | 1.34      | 1.75  | 118°    | 0°               | 46c |
| D. (ett)Rh <sub>2</sub> L <sub>6</sub> <sup>2+</sup>                                 | 6                               | 1.36      | 1.73  |         |                  | 45c |
| E. (ett)Co <sub>2</sub> Cp' <sub>2</sub>   | 6                               | 1.369     |       |         |                  | 45b |
| F. (ett)Ni <sub>2</sub> Cp' <sub>2</sub>   | 7                               | 1.360     | 1.718 |         | 0°               | 45a |
| G. (ett)Fe <sub>4</sub> L <sub>12</sub>  | 7                               | 1.332     | 1.775 | 101°    | 0°               | 12a |
| H. (ettMe <sub>2</sub> )Pt <sub>2</sub> X <sub>2</sub> L <sub>2</sub>                | 8                               | 1.34      | 1.75  | 120°    |                  | 46b |
| I. (ett)Cu <sub>2</sub> (C <sub>3</sub> OS <sub>4</sub> ) <sub>2</sub> <sup>2-</sup> | 8                               | 1.467     | 1.673 |         | 0°               | 46f |

<sup>a</sup> Except for G, all compounds listed possess dithiolene-like structure. <sup>b</sup> Number of d electrons is assigned assuming ett<sup>4-</sup> in the metal complexes.

ett (Table III), one is tempted to conclude that in most cases, it should be considered as a tetraanionic ligand with a C-C double bond. However, we postpone the discussion of this point until we have looked at the interaction of ett with different model fragments. Let us pay more attention to the composition of some of the ett ligand's orbitals.

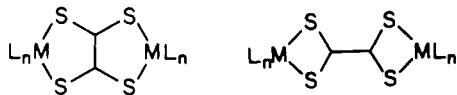
Most of the high-lying filled orbitals can be regarded as symmetry-adapted combinations of the sulfur lone pairs, three at each sulfur (two of  $\sigma$  and one of  $\pi$  type), but some deviations from this simple picture will appear later to be important in the study of the coordinating ability of ett. First, the  $2b_{1u}$  orbital is mainly localized at the carbon atom for electronegativity reasons. It is essentially the carbon-carbon  $\pi$  bond. Consequently, it will not contribute too much to the ligand's  $\pi$ -donor ability. Second,  $2b_{2u}$  is the antibonding combination of the in-plane  $\pi$  orbitals of each CS<sub>2</sub> moiety which, upon bending, became sulfur lone-pair orbitals. There is a slight but significant, and ultimately important hybridization apparent in the contour map of  $2b_{2u}$  (Figure 13). The orbital is more extended in the "dithiolene" region of ett than in the "dithiocarbamate" region. The definitions of these regions are obvious and are given in 43. Other in-plane lone-pair orbitals

**43**

are almost pure p orbitals and, consequently, have the same electronic density at both coordination sites (see, e.g.,  $2b_{1g}$  and  $2a_g$  in Figure 13).

### C<sub>2</sub>S<sub>4</sub> Complexes

In order to compare the two coordination modes available for ett, a dithiolene-like mode, 44, and a dithiocarbamate-like mode, 45, we shall first look at its interaction with an ML<sub>2</sub> fragment (modeled by NiH<sub>2</sub>). In Figure 14, such an interaction diagram

**44****45**

is presented for the dithiolene-like coordination of two ML<sub>2</sub> fragments with a bridging ett ligand. The orbital filling represented corresponds to a d<sup>8</sup> metal ion and the orbitals are labeled according to D<sub>2h</sub> symmetry.

The symmetric and antisymmetric combinations of the well-known a<sub>1</sub> and b<sub>1</sub> orbitals of both ML<sub>2</sub> fragments can interact with the appropriate combinations of sulfur  $\sigma$  lone pairs and create four bonding and four antibonding orbitals. The symmetric combination of the d<sub>xz</sub> orbitals, on the other hand, interacts with the

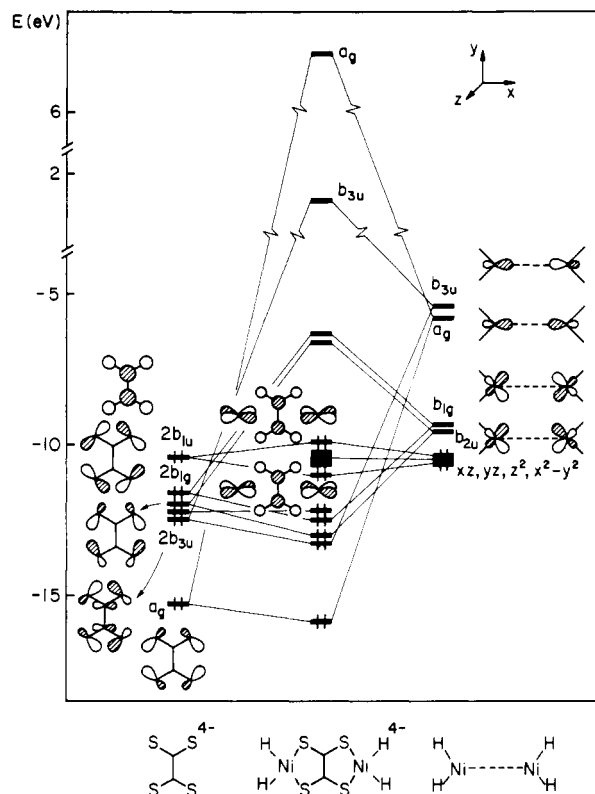


**Figure 14.** Interaction diagram of C<sub>2</sub>S<sub>4</sub><sup>4-</sup> with two ML<sub>2</sub> fragments in the dithiolene-like coordination mode.

HOMO ( $2b_{1u}$ ) of ett<sup>4-</sup>. This interaction, however, is not strong, since the carbon and sulfur contributions to the HOMO have opposite sign and the overall overlap with d<sub>xz</sub> is small.

The same pattern is found for the dithiocarbamate-like interaction diagram (Figure 15), except that the symmetries of the combination of the ML<sub>2</sub> orbitals are different because the ligand and the coordinate axes have been rotated. One also sees the same weak  $\pi$  interaction.

Although the interaction diagrams indicate that both isomers should be stable, the dithiolene-like coordination 44 is calculated to be more stable than the dithiocarbamate mode 45 by ~32 kcal/mol (i.e., ~8 kcal/mol per each Ni-S bond) for Ni(II). Similar values are found for Ni(III) and Ni(IV), always favoring the dithiolene-type coordination. The calculated equilibrium distances are presented in Table IV together with the experimental ones.

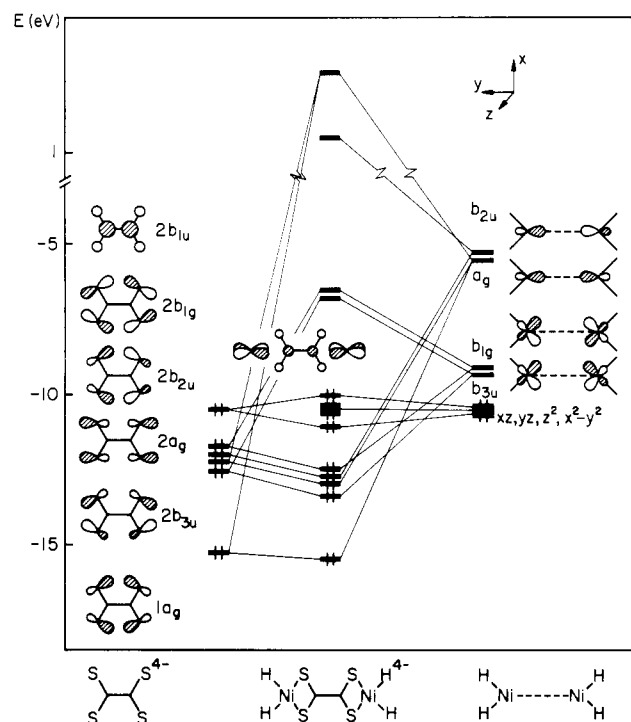
We have already commented on the difficulties associated with comparing the dithiocarbamate-like coordination of ett with the dithiocarbamates themselves, but two trends are evident from Table IV. The metal-sulfur bond is weaker for dithiocarbamates than it is for dithiolenes, and for both kinds of compounds, the bond is stronger for the lower electron counts.

To understand the effect of the oxidation state, look at either Figure 14 or Figure 15. The  $\pi^*(\text{M}-\text{L})$  orbital is filled for d<sup>8</sup> but becomes empty for d<sup>7</sup>, slightly strengthening the bond. The next

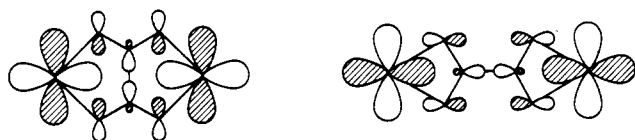
**Table IV.** Overlap Populations and Bond Distances Calculated for ett(NiL<sub>2</sub>)<sub>2</sub>, Compared with Experimental Values for Nickel Bisdithiolenes and Bisdithiocarbamates

|                      | oxidat state | Ni-S overlap populat |        |       | caled Ni-S dist | exptl Ni-S dist <sup>a</sup> |
|----------------------|--------------|----------------------|--------|-------|-----------------|------------------------------|
|                      |              | $\sigma$             | $\pi$  | tot   |                 |                              |
| dithiolene side      | +2           | 0.412                | 0.009  | 0.420 | 2.18            | 2.171                        |
|                      | +3           | 0.412                | 0.032  | 0.444 | 2.14            | 2.143                        |
|                      | +4           | 0.430                | 0.032  | 0.462 | 2.08            | 2.101                        |
| dithiocarbamate side | +2           | 0.327                | 0.0003 | 0.328 | 2.29            | [2.23] <sup>b</sup>          |
|                      | +3           | 0.327                | 0.027  | 0.354 | 2.25            |                              |
|                      | +4           | 0.348                | 0.027  | 0.375 | 2.18            |                              |

<sup>a</sup> Average from literature values. <sup>b</sup> Oxidation state definition for dithiocarbamates is different from that of dithiocarbamate-like ett (see text).

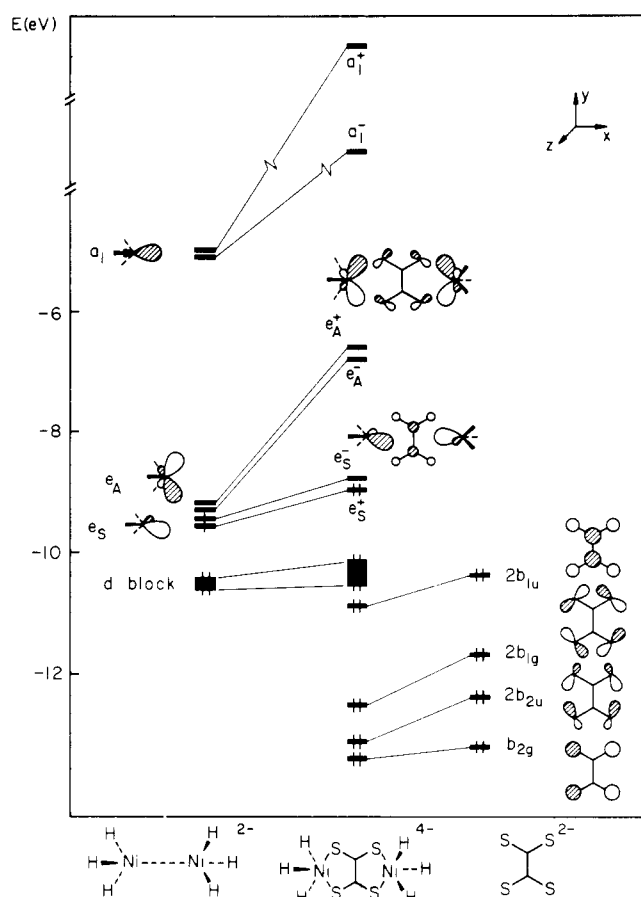
**Figure 15.** Diagram for the interaction of C<sub>2</sub>S<sub>4</sub><sup>4-</sup> with two ML<sub>2</sub> fragments in the dithiocarbamate coordination mode.

orbital to be emptied, for d<sup>6</sup>, is a combination of the two d<sub>x<sup>2</sup>-y<sup>2</sup></sub> orbitals, made antibonding by interaction with 2a<sub>g</sub>, **46**.

**46**

What is the orbital rationale for the greater stability of the dithiolene mode of coordination? The major effect comes from the a<sub>g</sub> interactions. The 1a<sub>g</sub> orbital of the ligand interacts with the same orbital of the M<sub>2</sub>L<sub>4</sub> composite in both coordination modes. However, as previously discussed, that orbital has greater electron density on the dithiolene side (Figure 13). Its overlap with the metal fragment orbital is 0.332 on that side but 0.266 at the dithiocarbamate side. The 2a<sub>g</sub> ligand orbital, on the other hand, is oriented to the dithiocarbamate side. But the overlap in this case is poor because of the opposite sign of the wave function at the carbon and the sulfur atoms (Figure 13). Hence, the interaction on this side is poorer (overlap integral = 0.138) than at the dithiocarbamate side (overlap = 0.178). The other  $\sigma$  interactions involve 2b<sub>1g</sub>, 2b<sub>2u</sub>, and 2b<sub>3u</sub>, and, again, they are greater on the dithiolene side, which can also be easily explained from the topology of the orbitals.

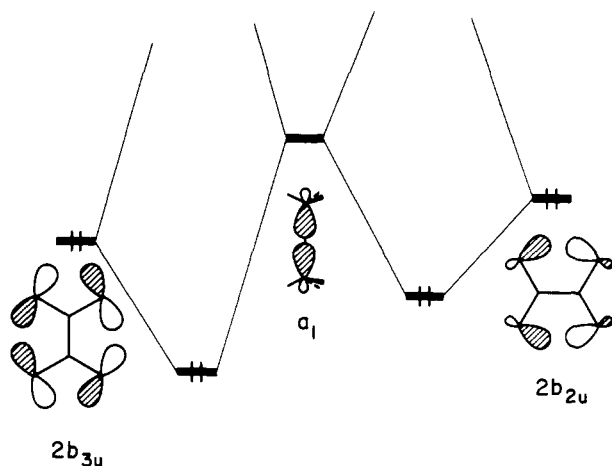
Only two ett complexes with ML<sub>2</sub> fragments are known so far (H and I in Table III). In one of them, two thiolato atoms are converted into thioether groups. The formal oxidation state of

**Figure 16.** Interaction diagram of C<sub>2</sub>S<sub>4</sub><sup>4-</sup> with two ML<sub>3</sub> fragments in a dithiolene-like coordination mode.

Pt in that compound is thus +2. Since the formation of  $\sigma$  S-Me bonds involves only the sulfur  $\pi$  lone pairs, the M-S bonding description of Figure 14 applies to this compound. Both the C-C bond distance and the nearly planar conformation of ett in this compound (Table III) indicate the existence of a carbon-carbon double bond. This should be expected when the 2b<sub>1u</sub> orbital of ett is occupied (Figure 14). The C-S bond distance is intermediate between typical values for a single (1.82) and a double (1.60) bond. In the other case, the ligand should clearly be considered as ett<sup>2-</sup> (i.e., tetrathiooxalato) with a C-C single bond and short C-S bonds. The striking difference in the structures of these two compounds with the same electron count can be understood in terms of the higher electronegativity of Cu, giving rise to a smaller HOMO/LUMO gap, hence a second-order Jahn-Teller distortion and depopulation of the ligand's 2b<sub>1u</sub> orbital.

Let us turn now to the coordination of C<sub>2</sub>S<sub>4</sub> to two ML<sub>3</sub> fragments. Of the two possible configurations, **47** and **48**, we choose the staggered one (**47**) which is the most symmetrical (C<sub>2h</sub>) since the inversion center of C<sub>2</sub>S<sub>4</sub> is preserved. It is also the structure found for the two binuclear compounds reported so far with ML<sub>3</sub> fragments.<sup>45</sup> The corresponding interaction diagram is shown in Figure 16.<sup>50</sup>





54

conclusion caused us some concern.

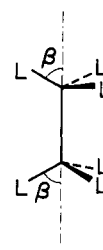
An additional result which we obtain is that electron density is located in the previously empty orbitals of the sawhorses. Some of them are metal-metal bonding ( $b_1$  and  $a_1$ ) and some metal-metal antibonding ( $a_2$  and  $b_2$ ). Thus, the metal-metal bond is expected to be of similar strength in both isomers. Numerical results indicate a slightly stronger bond for the dithiocarbamate mode.

To see how these results are reflected in the structure of related compounds, we can look first at  $\text{Fe}_2(\text{CO})_6(\text{acetylene})$ .<sup>52</sup> This is a Fe(0) compound and has the M-M bonding  $b_1$  orbital of the sawhorse filled. As a consequence, it has a shorter M-M bond distance (2.316 Å) than in the Fe(I) compound of **32** (2.486 Å). This fits well with their MO descriptions; a further difference is that the second-order Jahn-Teller effect observed in  $\text{Fe}_2(\text{CO})_6(\text{acetylene})$ <sup>51,52</sup> is not operative for **53**.

A comparison with an analogous dithiolene compound can also be illustrative: the calculated overlap populations for both isomers nicely correlate with bond distances in **53** (dithiocarbamate coordination mode) and in  $(\text{Ph}_2\text{C}_2\text{S}_2)\text{Fe}_2(\text{CO})_6$  (dithiolene coordinated to the same sawhorse), as shown in Table V.

We were concerned that our computations made the unobserved dithiolene-type complex more stable than its realized alternative. Therefore, several tests were made to check the validity of the calculated stabilities of both isomers. First, the SCS angle, taken as  $120^\circ$  in our calculations, was optimized for the dithiocarbamate isomer (SCS calculated =  $100^\circ$ ; experimental =  $101^\circ$ <sup>12a</sup>). Second, the orientation of the ligands in the sawhorses was optimized ( $\beta$  angle in **55**) for both isomers (calculated  $\beta \approx 30^\circ$  in both cases). Finally, a different set of parameters for Fe, taken from the literature, was tested.<sup>51</sup> In all cases, the dithiolene-like isomer appeared to be more stable. Therefore, we feel that this prediction that this isomer should be obtainable is a strong one, and the fact that the less stable isomer has been synthesized is not attributable to thermodynamic reasons but to kinetic ones. We would encourage any attempt to synthesize the unknown isomer.

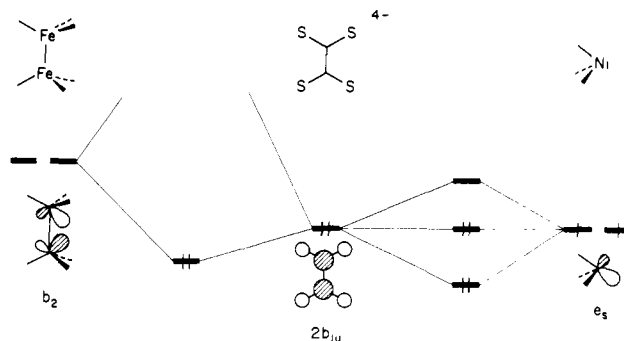
We note here again the recent remarkable synthesis of a 1:1 mixture of both dithiolene- and dithiocarbamate-like isomers of  $(\text{Cp}_2\text{Ti})_2\text{C}_2\text{S}_4$  by Harris and Dahl.<sup>45d</sup> For this  $\text{ML}_n$ , the two



55

isomers coexist, and so they should for other metal fragments coordinating to the versatile  $\text{C}_2\text{S}_4$  ligand.

After this lengthy discussion of the orbital interactions of ett with various metal centers, it should be clear that the description of that ligand as dianionic or tetraanionic is not easy. It depends on how much the ligand's  $2b_{1u}$  orbital is populated: the more populated it is, the closer we are to a  $\text{C}_2\text{S}_4^{4-}$  situation. This, in turn, is determined by several factors: (a) the more electronegative the metal is, the more it mixes with  $2b_{3u}$  and accepts electron density, provided it has six d electrons or less; (b) for the  $d^7$  and  $d^8$  compounds, filling the antibonding combination of  $2b_{1u}$  with the appropriate d orbital (essentially  $d_{xz}$ ) should have a still larger effect on the structure of ett; and (c) the  $\pi$ -acid character on the other ligands can also affect the amount of mixing. These trends are corroborated by the C-C and C-S bond distances presented above in Table III: The C-C distances are certainly shorter than a C-C single bond and quite close to a typical double bond distance, while the C-S distances are intermediate between those of a single bond ( $\sim 1.80$  Å) and a double bond ( $\sim 1.71$  Å). Perhaps two extreme cases are compounds F and G, Table III, which are isoelectronic ( $d^7$ ) yet the  $\text{Fe}_2\text{L}_{12}$  derivative is much closer to an  $\text{ett}^{4-}$  ligand and the  $\text{Ni}_2\text{Cp}_2'$  one is more like an  $\text{ett}^{2-}$  derivative. The interaction diagram for the first compound can provide an explanation (Figure 17): the  $e_A$  orbitals of the  $d^7$   $\text{ML}_3$  fragments have one unpaired electron each and can accept, at most, two electrons from ett. On the other hand, in a  $\text{M}_2\text{L}_6$  sawhorse, the  $e_A$  orbitals form a metal-metal bonding orbital, which is full for a  $d^7$  metal, and an empty, metal-metal antibonding one. This is illustrated in **56**. For the sawhorses in **53**,



56

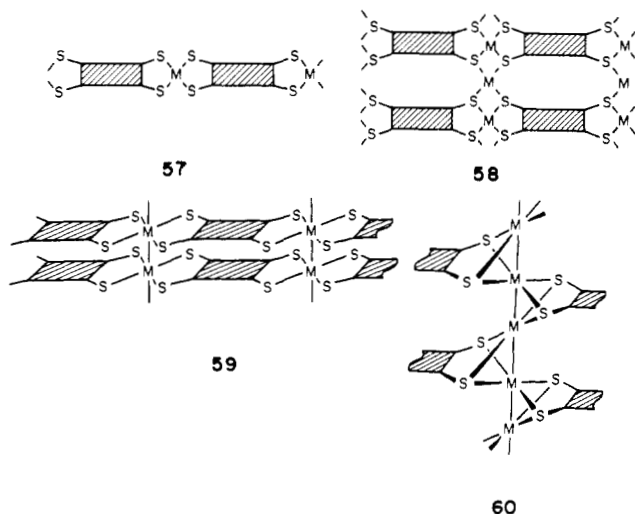
then, there are two empty orbitals well suited to accept electron density from  $\text{ett}^{4-}$  and transform it, formally, into  $\text{ett}^{2-}$ . The computed net charges on ett, the C-C and the C-S overlap populations (Table VI) show a consistent description of this difference.

#### One- and Two-Dimensional Metal Derivatives of ett

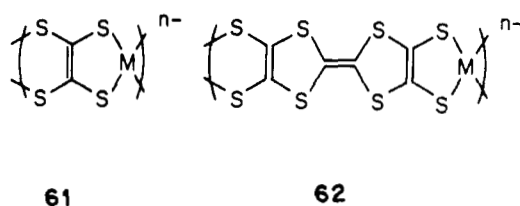
We have previously commented on the structures of discrete compounds that suggest one- and two-dimensional structures **57-60**. The shaded rectangle represents the central  $\text{C}_2$  fragment of an ett ligand in either of its possible coordination modes, or the  $\text{C}_4$  backbone of the tetrathiosquarato dianion (ttsq) **4**. Let us see what is known about the polymers themselves.

Polymeric metal complexes of both the ethylenetetrathiolate (ett) ligand **61** and tetrathiofulvalenetetrathiolate (tftt) **62**, where

(52) Cotton, F. A.; Jamerson, J. D.; Stults, B. R. *J. Am. Chem. Soc.* **1976**, *98*, 1774.

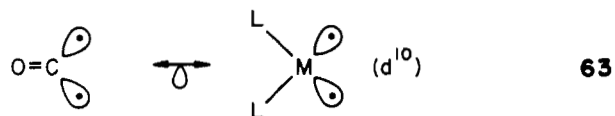


$n = 0, 1,$  and  $2,$  have been prepared and found to be nonstoichiometric. They are also quite good electrical conductors, with

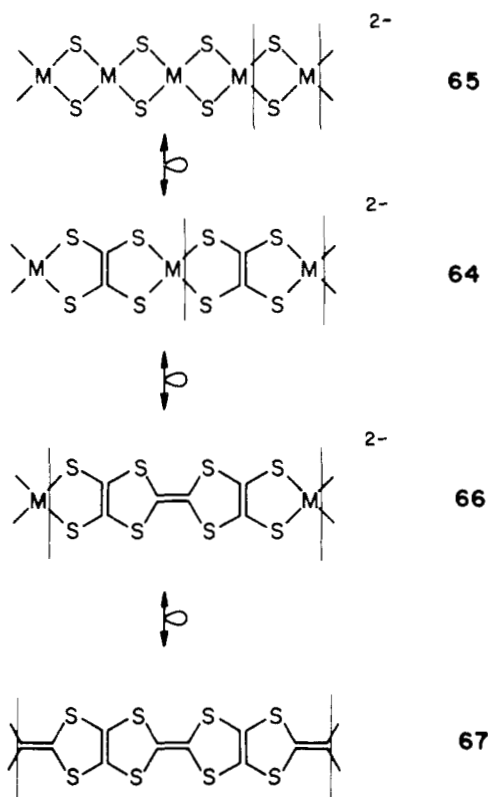


room-temperature compaction conductivities of up to  $20 \Omega^{-1} \text{cm}^{-1}$ .<sup>47,53,54</sup> The structure of these polymers is as yet undetermined. However, the closely related metal oxalates are known to form planar ribbons, usually with additional ligands (typically  $\text{H}_2\text{O}$  or  $\text{NH}_3$ ) in the axial positions,<sup>55a-d</sup> as do some dithiooxalato polymers.<sup>55e</sup>

Using the isolobal analogies 63<sup>56</sup> and 35, we find support for the existence of such a planar ribbon and also suggestions for other exciting structures. Let us consider our hypothetical ribbon of

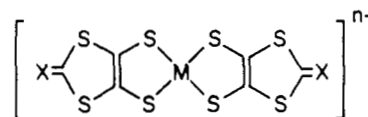


$\text{M}(\text{ett})$  64 where the charges correspond to a  $d^8$  transition-metal dication (Ni, Pd, and Pt). If the  $\text{C}_2$  fragments are replaced by the isolobal  $\text{M}^{2+}$  ( $d^8$ ), the anionic ribbons of stoichiometry  $\text{MS}_2^{2-}$  65 are generated. Several such ribbons are known ( $\text{Na}_2\text{PdS}_2$ ,  $\text{Na}_2\text{PtS}_2$ ,  $\text{H}_2\text{PtS}_2$ ,  $\text{Rb}_2\text{PtS}_2$ , and  $\text{BaPdS}_2$ ),<sup>57</sup> and all but the last are planar. A theoretical account of these compounds has been presented.<sup>58</sup> If instead we replace each other  $\text{M}^{2+}$  ion in 64 by its isolobal analogue  $\text{C}_2^{4+}$ , we get the chain 66 with tftt as a ligand. Further replacement of metal ions yields the isolobal organic chain



67. We are not aware of any such organic ribbon, but some oligomers are certainly known.<sup>59</sup>

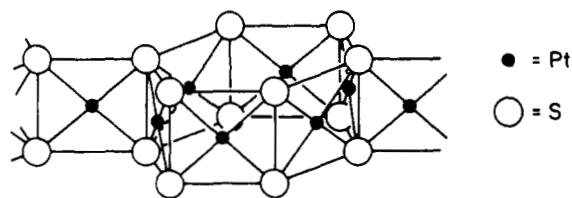
On the other hand, the structure of 68 has been determined for  $\text{X} = \text{S}$  and  $\text{M} = \text{Ni}$ ,  $n = 0.29$  and  $0.5$ . These are also planar compounds.<sup>6f,g</sup> Using the isolobal analogy 63, we can convert



68

it on paper into a trinuclear precursor of the polymer 64. We have thus generated a collection of ribbons, ranging from the purely inorganic 65 to a purely organic 67.

Another nonplanar structure of a different stoichiometry  $\text{M}_2(\text{ett})$ , 60, is suggested by the molecular compounds already discussed. There are a couple of two-dimensional analogues with the same type of honeycomb structure 69:  $\text{A}_2\text{M}_3\text{S}_4$  ( $\text{A} = \text{Rb}$  and



69

$\text{Cs}$ ;  $\text{M} = \text{Pd}$  and  $\text{Pt}$ ).<sup>60</sup> In these compounds, the metal-metal distances are in the range  $3.1\text{--}3.2 \text{ \AA}$ , indicative of a weak in-

(53) Martínez Rivera, N.; Engler, E. M.; Schumaker, R. R. *J. Chem. Soc., Chem. Commun.* **1979**, 184.

(54) (a) Ribas, J.; Cassoux, P. C. *R. Hebd. Seances Acad. Sci., Ser. C* **1981**, 293 II, 665. (b) Reynolds, J. R.; Karasz, F. E.; Lillya, C. P.; Chien, J. C. W. *J. Chem. Soc., Chem. Commun.* **1985**, 268.

(55) (a) Wroblewski, J. T.; Brown, D. B. *Inorg. Chem.* **1979**, 18, 2738. (b) Mazzi, C.; Caravelli, F. *Period. Mineral.* **1957**, 26, 2. (c) Garaj, J.; Langfelderová, H.; Lundgren, G.; Gažo, J. *Collect. Czech. Chem. Commun.* **1972**, 37, 3181. (d) Verdaguer, M.; Julve, M.; Michalowicz, A.; Kahn, O. *Inorg. Chem.* **1983**, 22, 2624. (e) Gleizes, A.; Verdaguer, M. *J. Am. Chem. Soc.* **1984**, 106, 3727.

(56) Silvestre, J.; Hoffmann, R., to be published.

(57) (a) Bronger, W.; Günther, O. *J. Less-Common Met.* **1972**, 27, 73. (b) Bronger, W.; Günther, O.; Huster, J.; Spangenberg, M. *J. Less-Common Met.* **1976**, 50, 49. (c) Bronger, W. *Angew. Chem., Int. Ed. Engl.* **1981**, 20, 52. (d) Bronger, W., private communication.

(58) Underwood, D. J.; Nowak, M.; Hoffmann, R. *J. Am. Chem. Soc.* **1984**, 106, 2837.

(59) Engler, E. M.; Lee, V.-Y.; Schumaker, R. R.; Parkin, S. S.; Greene, R. L.; Scott, J. C. *Mol. Cryst. Liq. Cryst.* **1984**, 107, 19.

(60) (a) Huster, J.; Bronger, W. *J. Solid State Chem.* **1974**, 11, 254. (b) Günther, O.; Bronger, W. *J. Less-Common Met.* **1973**, 31, 255.



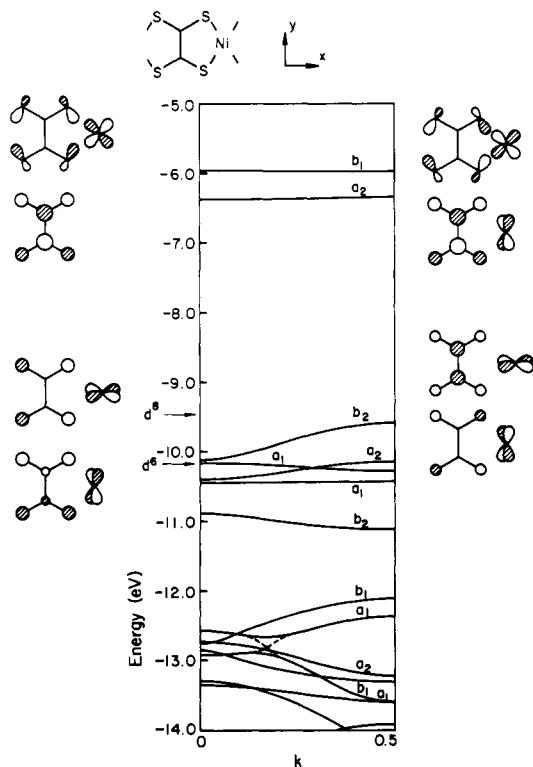
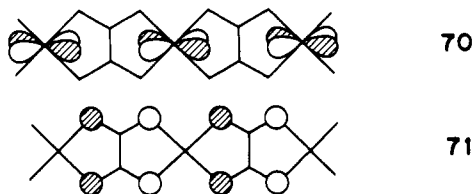
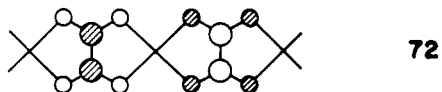


**Figure 18.** Band structure for a planar Ni(ett) ribbon in the dithiolene-like coordination mode.

the direct overlap of their d orbitals. However, the in-phase combination ( $k = 0$  in Figure 18) of the  $d_{xz}$  orbitals **70** has the same symmetry properties as that of the  $b_{2g}$  orbitals of ett, **71**.



The out-of-phase combination ( $k = 0.5$ ) of  $d_{xz}$  has the same symmetry as that of the  $2b_{1u}$  ett orbitals **72**. Hence,  $d_{xz}$  mixes



with  $b_{2g}$  for  $k = 0$  but with the higher-lying  $2b_{1u}$  for  $k = 0.5$ . Its energy is consequently lower for  $k = 0$  than it is for  $k = 0.5$ . Also the crystal orbital at  $k = 0$  is largely (90%)  $d_{xz}$ , while it has nearly equal contributions of  $d_{xz}$  and  $2b_{1u}$  at  $k = 0.5$ , because of the better energy match in the latter case. A similar explanation applies for the  $a_2(d_{yz})$  band.

The mechanism through which the nonoverlapping orbitals on neighboring unit cells produce a wide band might be regarded as the solid-state equivalent of through-bond coupling in molecules<sup>61</sup> but is governed now by translational symmetry in addition to group symmetry.

The band structure of the dithiocarbamate-like isomer (Figure 19) is quite similar, except that each metal orbital interacts with different ligand orbitals. The poorer interaction previously discussed for the dithiocarbamate side of the ligand has some interesting consequences. First, the  $d_{xy}$  orbital is much less destabilized, and the direct band gap for a  $d^8$  compound is decreased to 2.4 eV. This fact would be reflected in different absorption spectra (hence color) of both isomers; also, the dispersion of this

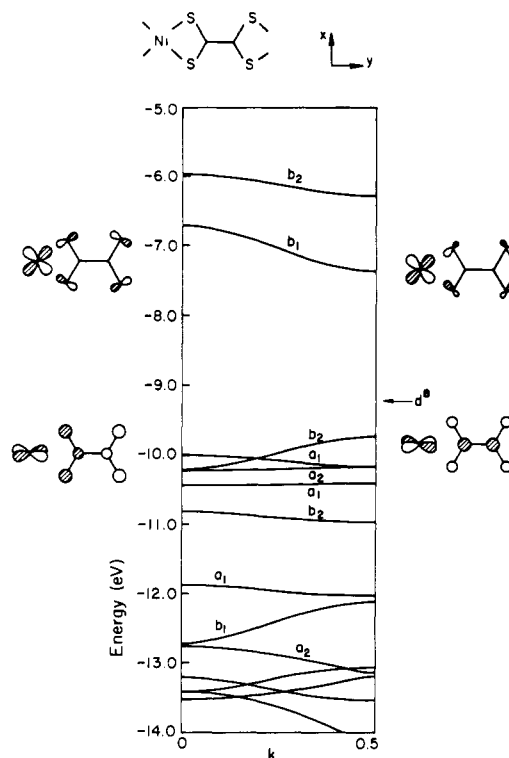


**Figure 19.** Band structure for a planar Ni(ett) ribbon in the dithiocarbamate-like coordination mode.

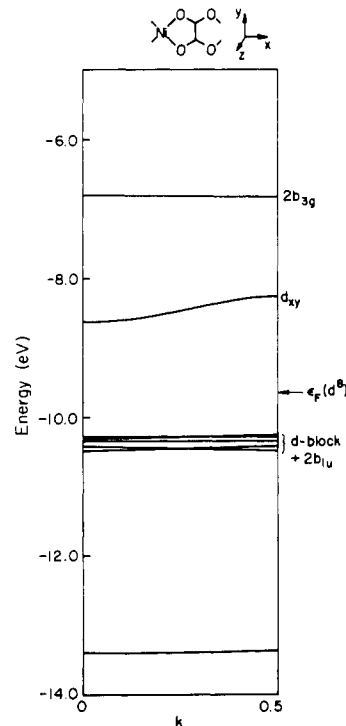
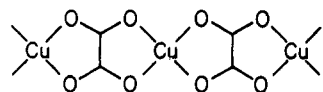


**Figure 20.** Band structure for a planar Ni(ox) ribbon with structure **73**.

band due to through-bond coupling guarantees a larger electron mobility in this case. This should make the dithiocarbamate-like isomer a better electrical conductor. On the other hand, as the  $\pi$  interaction is also poorer in this coordination mode, the  $d_{xz}$  band is lower in energy and overlaps with the rest of the d bands. This suggests the possibility that a  $d^6$  compound could present metallic conductivity.

A look at the band structure of the well-known oxalato ribbons **73** should prove instructive. Since the oxygen is more electronegative than sulfur, on substituting oxygen for sulfur in ett to give oxalato (abbreviated ox), the mixing of the atomic orbitals

(61) Hoffmann, R. *Acc. Chem. Res.* **1971**, *4*, 1.

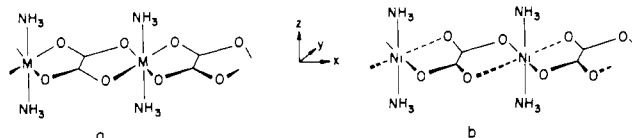


73

of the donor atoms with those of  $C_2$  and the metal is drastically decreased. Hence, the bands show much less dispersion, as calculated for a  $Ni(ox)$  ribbon (Figure 20). Now the narrow  $d_{xy}$  band (bandwidth = 0.36 eV) is the conduction band for a  $d^8$  compound (counting the oxalato ligand as dianionic), and their partially reduced derivatives might behave as metals with conductivities smaller than the corresponding ett derivatives. For less d electrons, the localized nature of the lower d bands should produce semiconductors, even for partially reduced (or oxidized) compounds.

For  $Cu(ox) \cdot \frac{1}{3}H_2O$ , which presents this structure,<sup>62</sup> the unpaired electron of each copper atom will be placed in the  $d_{xy}$  band. Depending on the relative magnitude of the bandwidth and the inter-electron repulsion, a metallic state susceptible of a Peierls distortion or an antiferromagnetic state may be produced.<sup>63</sup> This is very much related to the low spin-high spin dichotomy in coordination compounds, the narrow bands favoring the antiferromagnetic insulator state with largely localized electrons, and the wide bands favoring the metallic diamagnetic state. Even though the one-electron formalism used doesn't allow us to decide whether a metallic or an antiferromagnetic state will be more stable, a simple comparison of the  $d_{xz}$  bandwidths found for ett and ox ribbons (0.54 and 0.36 eV, respectively) tells us that the chances for a metallic state are larger for the ett ribbon, while the oxalato ribbon is more likely to be antiferromagnetic, as experimentally found.<sup>64</sup> As Girerd et al. proposed based on calculations on a dimer,<sup>64a</sup> the addition of two axial ligands to the metal atom in the oxalato ribbon puts the unpaired electron in the  $d_{z^2}$  band. In this case, this band is above  $d_{xy}$ . Since the  $d_{z^2}$  band is narrower due to the smaller overlap of  $d_{z^2}$  with the ligand orbitals (0.22 eV is the bandwidth calculated for our model  $Ni(ox)$  with two axial  $NH_3$  ligands), the electrons are more localized and the antiferromagnetic coupling constant is significantly smaller for  $Cu(ox)(NH_3)_2 \cdot 2H_2O$ .<sup>55c,64a</sup>

As can be deduced from Figure 21, due to the small energy difference between the  $d_{z^2}$  and  $d_{xy}$  bands, the  $NiL_2(ox)$  compounds, **74a**, can be paramagnetic, also with antiferromagnetic coupling.<sup>65</sup>



74

Furthermore, a second-order Peierls distortion might be expected due to the small band gap. A distortion such as **74b** destroys the  $xz$  symmetry plane, allowing the  $x^2-y^2$  and  $z^2$  bands to mix and leading to net stabilization for  $d^7$ ,  $d^8$  (low spin) and  $d^9$  electron configurations. The ESR spectra of  $d^7$  compounds  $[Co(oxalate)L_2]_n$  indicate the presence of a rhombic distortion;<sup>65</sup> a distortion

(62) Michalowicz, A.; Girerd, J. J.; Gordon, J. *Inorg. Chem.* **1979**, *19*, 3004.

(63) (a) Whangbo, M.-H. *J. Chem. Phys.* **1980**, *73*, 3854. (b) Whangbo, M.-H. *J. Chem. Phys.* **1981**, *75*, 4983. (c) Whangbo, M.-H. *Acc. Chem. Res.* **1983**, *16*, 95 and references therein.

(64) (a) Girerd, J. J.; Kahn, O.; Verdager, M. *Inorg. Chem.* **1980**, *19*, 274. (b) Dubciki, L.; Harris, C. M.; Kokot, E.; Martin, R. L. *Inorg. Chem.* **1966**, *5*, 93. (c) Figgis, B. N.; Martin, D. J. *Inorg. Chem.* **1966**, *5*, 100. (d) McGregor, K. T.; Soos, Z. G. *Inorg. Chem.* **1976**, *15*, 2159. (e) Jotham, R. W. *J. Chem. Soc., Chem. Commun.* **1973**, 178.

(65) Van Kralingen, C. G.; Van Ooijen, J. A. C.; Reedijk, J. *Transition Met. Chem.* **1978**, *3*, 90.

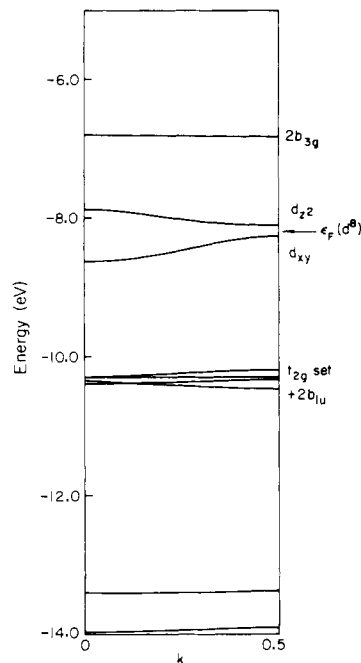
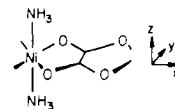


Figure 21. Band structure for a  $Ni(ox)(NH_3)_2$  ribbon with structure **74**.

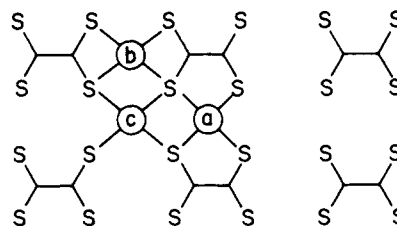
is clear also in the structure of the  $d^9$  copper chain  $[Cu(oxalate)(NH_3)_2]_n$ , presenting two short (2.147 Å) and two long (2.327 Å) Cu-O bonds.<sup>55c</sup>

On the other hand, the position of the  $d_{z^2}$  band above or below the  $d_{xy}$  one will largely depend on the relative strength of the equatorial and axial metal-ligand interactions. For a  $d^7$  compound, the unpaired electron may occupy the  $d_{z^2}$  band and produce poor antiferromagnetic coupling, as observed in a series of  $CoL_2ox$  compounds<sup>66</sup> where  $J = -9 \sim -11 \text{ cm}^{-1}$ .

For the Fe(II) compounds ( $d^6$ ), the  $t_{2g}$  bands are full and the only available conduction mechanism is thermal activation of the valence electrons to the conduction band, in agreement with the small conductivity found for  $Fe(H_2O)_2ox$  ( $< 10^{-10} \Omega^{-1} \text{ cm}^{-1}$ ).<sup>67</sup> When this compound is partially oxidized, the conductivity is enhanced to  $\sim 10^{-4} \Omega^{-1} \text{ cm}^{-1}$ . Clearly a band that is not wide has been partially emptied, and the increased conductivity could be attributed to a much more facile electron hopping mechanism.

### Two-Dimensional Complexes of ett

If ett ligands are arranged in a two-dimensional array, **75**, a metal ion can occupy three different sites (a, b, and c). For a compound of stoichiometry  $ML$ , only the occupation of the sites



75

(66) (a) Blomquist, D. R.; Hansen, J. J.; Landee, C. P.; Willett, R. D.; Buder, R. *Inorg. Chem.* **1981**, *20*, 3308. (b) Barros, S. de S.; Friedberg, S. A. *Phys. Rev.* **1966**, *141*, 637.

(67) Wroblewski, J. T.; Brown, D. B. *Inorg. Chem.* **1979**, *18*, 2738.

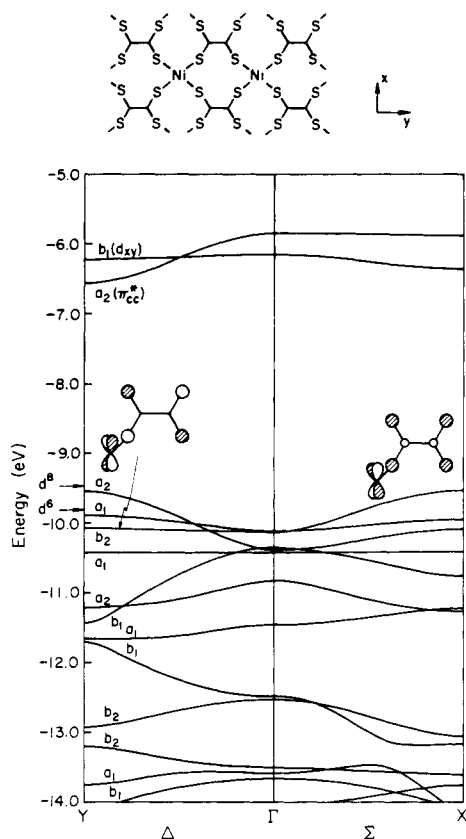


**Figure 22.** Band structure for a layered Ni(ett) compound, with Ni occupying the position c in **75**.

c may produce a polymeric two-dimensional structure. How likely is this structure?

The calculated band structure for such a network is plotted along the high-symmetry lines in Figure 22. If compared with that for the one-dimensional compound with the metal atoms occupying the a sites in **75** (Figure 18), it looks very similar along the  $\Gamma X$  line, but much larger dispersion arises along the  $\Gamma Y$  line. In particular, the band generated from the  $d_{xz}$  orbital produces a large dispersion via the previously noted through-bond coupling, and as a result, compounds with less than eight d-electrons should behave as metals. The same feature appears with the metal atoms in a. This leads to the conclusion that the lateral contacts between ribbons may play an important role in determining the electrical properties of these compounds, as found for the inter-stack contacts in dithiolenes above. Can these compounds be expected to be stable?

The metal d orbitals interact in this case with  $b_{1g}$ ,  $b_{3u}$ , and  $b_{2u}$  of ett and not with  $2b_{1g}$ ,  $2b_{2u}$ , and  $2b_{3u}$  as in the one-dimensional ribbon. A look at the MO diagram of ett (Figure 12) tells us that the ett donor orbitals involved in our two-dimensional structure are much poorer donors, since they are much lower in energy. As a result, structure **75** with the a sites occupied by the metal atoms is more stable by 1.35 eV per unit cell than an isomeric net with the metals in c sites. This is due to the smaller Ni-S overlap population, which falls from 0.455 to 0.206, respectively. This is best seen in Figure 23, where the density of states is plotted for both cases. In the one-dimensional case, a large part of the density on the sulfur atoms is below -14.0 eV, since several sulfur lone pairs are stabilized through interaction with the metal orbitals. For the two-dimensional structure, a larger part of the sulfur orbitals remains at relatively high energy, since these orbitals are little stabilized by the interaction with the metal atoms. In addition, the structure with the metal atoms in a can avoid the S-S repulsive interactions between ribbons by increasing the distance between them or by some type of sliding or tilting as those seen for dithiolenes. The two-dimensional structure **75** with metal atoms occupying the c sites is therefore an unlikely one for a compound of stoichiometry  $M(ett)$  ( $M = d^6-d^8$ ).

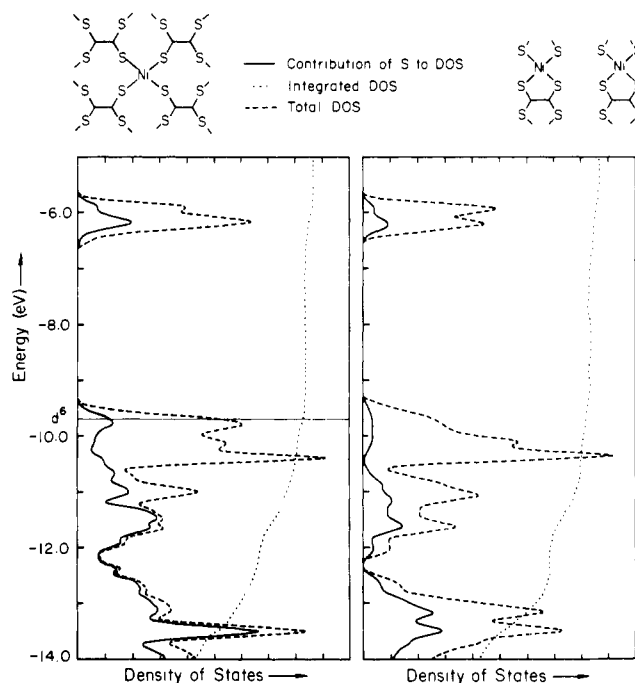
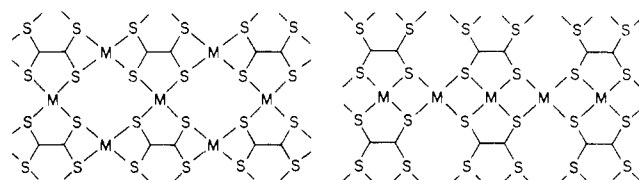


**Figure 23.** Density of states (dashed lines) and the sulfur contribution to the DOS (solid line) in two  $M(ett)$  two-dimensional layers. At left is the DOS for the dithiolenes a-type layer (see **75**). At right we have the same for a c-type ordering.

Still, with the planar arrangement of ett ligands shown in **75**, three isomers of stoichiometry  $M_2L$  are possible. We will explore those with metal atoms occupying sites a and c, **76**, or a and b,



76

77

**77**, simultaneously. Ni(II) would give now a neutral compound.

The band structure for the  $M_2L$  isomer **76**, a + c, is presented in Figure 24. In essence, four new d bands are added to the previous diagrams in the valence region and one in the conduction zone. The latter band is strongly mixed with the previously found  $d_{xy}$  band, producing large dispersion in the conduction zone and substantially decreasing the band gap, which is now  $\sim 1.3$  eV. This change can be viewed as the band equivalent of a three-orbital interaction, as schematically represented in **78**. Consequently, a  $d^8 M_2(ett)$  derivative with this structure should be a better semiconductor than a  $d^8$  ribbon compound  $M(ett)$ , and a marked red shift in the absorption spectrum is to be expected for the addition of the second metal atom. For the same reasons discussed above, the Ni-S bond in the c site should be weaker than that in site a.

For  $d^7$  compounds, metallic behavior can be expected, and the metallic state is likely to be stable toward a Peierls distortion.

A metal dithiolenes of formula  $Cu[Ni(mnt)]_2$  which shows high conductivity ( $5 \times 10^{-2} \Omega^{-1} \text{cm}^{-1}$ ) at room temperature, with an activation energy of 0.05 eV (corresponding to a band gap of 0.1 eV),<sup>68a</sup> might well have a related structure **79**, analogous to that

(68) (a) Manecke, G.; Wöhrl, D. *Makromol. Chem.* **1968**, *116*, 36. (b) Weiss, J. *Angew. Chem., Int. Ed. Engl.* **1984**, *23*, 225. (c) Holdcroft, G. E.; Underhill, A. E. *Synth. Met.*, submitted.



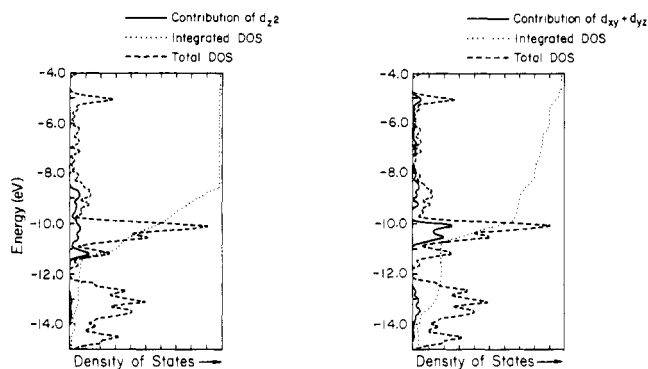


**Figure 26.** Density of states and the contributions of some d orbitals in  $M_2(\text{ett})$  **9**.

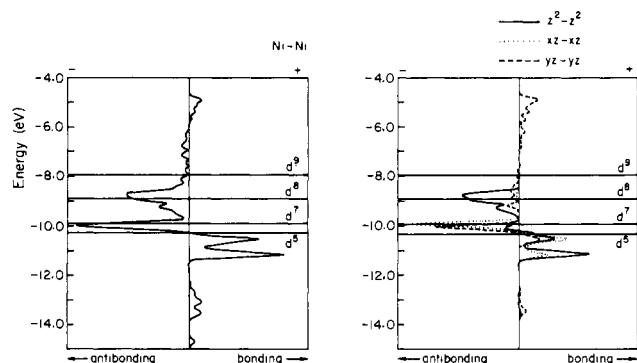


**Figure 27.** COOP curves for the Ni-Ni bond (left),  $d_{z^2}/d_{z^2}$  (right, solid line),  $d_{xz}/d_{xz}$  (right, dotted line), and  $d_{yz}/d_{yz}$  (right, dashed line).

Other than the general features just outlined, it is not easy to extract much structural information from the raw data of Figure 25. If the band structure information is presented as a density of states plot (Figure 26), the contribution of the  $d_{z^2}$  to the density of states shows that these orbitals are spread over a 3 eV energy range due to metal-metal interaction. The contributions of  $d_{xy}$  and  $d_{yz}$  show a larger dispersion, due to their  $\sigma$  interaction with the ligand orbitals. The next question to answer is, which of these states are bonding and which are antibonding?

The COOP (Crystal Orbital Overlap Population) curves<sup>70</sup> (Figure 27) show that the bands that are metal-metal bonding are the ones which are filled with the first ten d electrons. The degree of metal-metal bonding is maximum for  $d^5$  and quite weak for  $d^8$  metals, the interaction becoming repulsive for a  $d^9$  compound. The M-M distances in the isolobal  $A_2M_3S_4$  compounds are 3.1–3.2 Å,<sup>60</sup> too long to be considered a bond but certainly shorter than in weakly interacting stacks that give rise to band formation and electrical conductivity (Table I). This is in excellent agreement with the qualitative predictions of Figure 25. Similar  $M(d^8)$ - $M(d^8)$  interactions with bridging donor atoms are also known for bi- and trinuclear compounds.<sup>71</sup> We calculate that the Ni-S bond is almost insensitive to the band filling, as should be expected for any metal-ligand bond in square-planar complexes. The differences in calculated energies between this structure and the planar two-dimensional one discussed above are very small (0.1–0.2 eV), and there is the possibility that both could be obtained through different synthetic routes.

### Extended Metal-Tetrathiosquarato Systems

Polymeric tetrathiosquarato (ttsq) complexes of the nickel group metals were prepared by Götzfried et al.<sup>72</sup> These polymers possess

(70) (a) Hughbanks, T.; Hoffmann, R. *J. Am. Chem. Soc.* **1983**, *105*, 3258. (b) Kertesz, M.; Hoffmann, R. *J. Am. Chem. Soc.* **1984**, *106*, 3453. (c) Saillard, J.-Y.; Hoffmann, R. *J. Am. Chem. Soc.* **1984**, *106*, 2006.

(71) (a) Cotton, F. A.; Han, S. *Rev. Chim. Miner.* **1983**, *20*, 496. (b) Piovesana, O.; Bellitto, C.; Flamini, A.; Zanazzi, P. F. *Inorg. Chem.* **1979**, *18*, 2258.

(72) Götzfried, F.; Beck, W.; Lurf, A.; Sebal, A. *Angew. Chem., Int. Ed. Engl.* **1979**, *18*, 463.

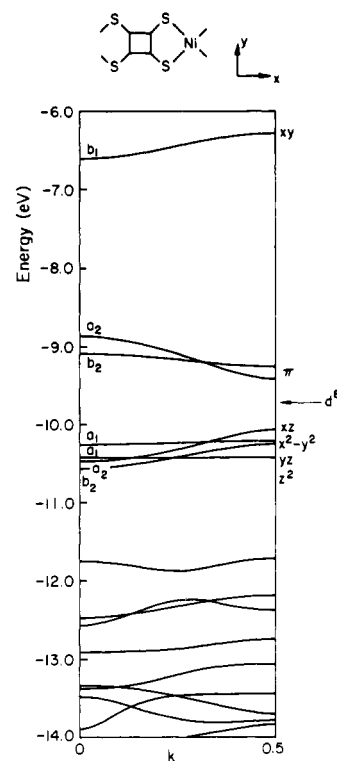
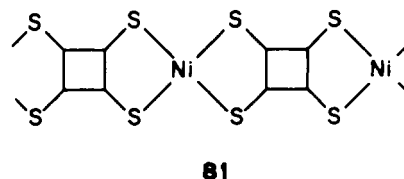


**Figure 28.** Band structure of a planar ribbon Ni(ttsq).

conductivities of  $10^{-4}$ – $10^{-7}$   $\Omega^{-1}$   $\text{cm}^{-1}$  at room temperature. Again, their structures are not known, but those of a binuclear gold compound<sup>73</sup> and of binuclear compounds of the related ligands squarato<sup>74</sup> and dithiosquarato are all planar,<sup>75</sup> as is the potassium salt of tetrathiosquarate itself.<sup>76</sup>

The band structure calculated for a Ni(ttsq) ribbon, **81** (Figure 28), is quite similar to that found for Ni(ett) ribbons (Figure 28). For a  $d^8$  metal, the d bands are full and the conduction bands ( $a_2$



and  $b_2$  at  $\sim -9$  eV) are formed by the  $e(\pi)$  orbitals of the ligand, split due to their different interaction with the metal d orbitals. The band gap is 0.65 eV. For lower electron counts, metallic conductivity could appear due to band overlap.

An INDO band calculation on the same systems has recently been reported.<sup>77</sup> The ligand orbitals' contributions to the valence and conduction bands are similar to our results, but no significant contribution of the metal d orbitals to them is found in the INDO calculations. Another difference between those results and the ones reported here is the magnitude of the band gap (5.85 eV at the INDO level).

The planar two-dimensional structure **7** is unlikely for geometrical reasons, but a structure of type **9** is possible. Also structures with a large degree of metal clustering such as the one found for  $[\text{Cu}_8(\text{dtsq})]_6^{4-}$  ( $\text{dtsq}$  = dithiosquarato),<sup>78</sup> are possible.

(73) Jones, P. G.; Sheldrick, G. M.; Fügner, A.; Götzfried, F.; Beck, W. *Chem. Ber.* **1981**, *114*, 1413.

(74) Simonsen, O.; Toftlund, M. *Inorg. Chem.* **1981**, *20*, 4044.

(75) Coucouvanis, D.; Hollah, D. G.; Hollander, F. G. *Inorg. Chem.* **1975**, *14*, 2657.

(76) Allmann, R.; Debaerdemaeker, T.; Mann, K.; Matusch, R.; Schmiedel, R.; Seitz, G. *Chem. Ber.* **1976**, *109*, 2208.

(77) (a) Böhm, M. C. *Phys.* **1983**, *122B*, 302. (b) Böhm, M. C. *Phys. Status Solidi* **1984**, *121*, 255.

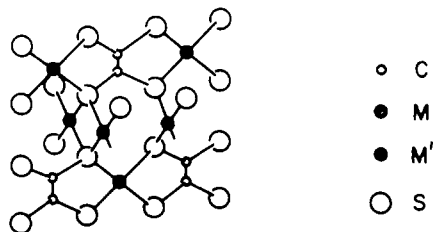
(78) (a) Hollander, F. J.; Coucouvanis, D. *J. Am. Chem. Soc.* **1974**, *96*, 5646. (b) Hollander, F. J.; Coucouvanis, D. *J. Am. Chem. Soc.* **1977**, *99*, 6268.

Table VII. Extended Hückel Parameters

| atom | orbital | $H_{ij}$ , eV | $\zeta_i(C_i)$ |               |
|------|---------|---------------|----------------|---------------|
| H    | 1s      | -13.60        | 1.30           |               |
| C    | 2s      | -21.40        | 1.625          |               |
|      | 2p      | -11.40        | 1.625          |               |
| O    | 2s      | -32.30        | 2.275          |               |
|      | 2p      | -14.80        | 2.275          |               |
| S    | 3s      | -20.00        | 1.82           |               |
|      | 3p      | -13.30        | 1.82           |               |
|      | 3d      | -9.00         | 5.35 (0.5366)  | 1.80 (0.6678) |
| Fe   | 4s      | -6.70         | 1.90           |               |
|      | 4p      | -3.53         | 1.90           |               |
|      | 3d      | -10.58        | 5.75 (0.5681)  | 2.00 (0.6294) |
| Ni   | 4s      | -7.34         | 2.10           |               |
|      | 4p      | -3.74         | 2.10           |               |
|      | 5d      | -10.08        | 6.01 (0.6333)  | 2.70 (0.5512) |
| Pt   | 6s      | -7.56         | 2.55           |               |
|      | 6p      | -4.32         | 2.55           |               |

The study presented here is not exhaustive, and other interesting possibilities might be sought, including the sheet structures **8** with metal-over-metal stacking analogous to the well-known platinum oxalates,<sup>79</sup> or a similar structure with metal-over-sulfur stacking, somewhat related to the stacking pattern found in several copper oxalates.<sup>36</sup>

Isolobal with PtS and PdS, the cooperite structure<sup>80</sup> would be a  $M'M_2(\text{ett})$  compound consisting of  $M'(\text{ett})^{2-}$  ribbons ( $d^8$ -M) cross-linked by  $M^+(d^8)$  ions, **82**. Other exotic and fascinating



## 82

(79) (a) Williams, J. M.; Schultz, A. J.; Underhill, A. E.; Carneiro, K. In "Extended Linear Chain Compounds"; Miller, J. S., Ed.; Plenum Press: New York, 1982; Vol. 1, Chapter 3. (b) Kobayashi, H.; Kobayashi, A. In "Extended Linear Chain Compounds"; Miller, J. S., Ed.; Plenum Press: New York, 1982; Vol. 2, Chapter 6.

(80) Wells, A. F. "Structural Inorganic Chemistry", 5th ed.; Clarendon Press: Oxford, 1984, p 755.

ways of arranging the isolobal  $\text{PdSe}_4^{2-}$  units were recently reported by Keszler and Ibers<sup>81</sup> in  $\text{Nb}_2\text{PdSe}_3$  and related compounds.

**Acknowledgment.** We are grateful to a grant from the Ministerio de Educación y Ciencia which made the stay at Cornell of Santiago Alvarez possible. Our research was supported by the National Science Foundation through research Grant CHE 8406119. Our work was greatly helped by communication with A. Underhill, A. Kobayashi, and L. Dahl, who provided us with much useful information prior to publication. Enric Canadell and Jerome Silvestre carefully read our manuscript, and for this we thank them, as well as Eleanor Stagg for the typing and Jane Jorgensen and Elisabeth Fields for the numerous drawings.

## Appendix

**Computational Details.** The standard geometries used for edt and ett consisted of  $120^\circ$  angles and bond distances  $\text{C-C} = 1.34 \text{ \AA}$  and  $\text{C-S} = 1.70 \text{ \AA}$ . The metal-sulfur distances, taken from the experimental data, were 2.22 (Fe and Ni) and 2.27  $\text{ \AA}$  (Pt).

The extended Hückel methodology<sup>82</sup> with weighted  $H_{ij}$ 's<sup>83</sup> was applied to molecules, and extended Hückel tight binding calculations<sup>84</sup> were used for polymers.

The parameters employed are presented in Table VII; the  $H_{ij}$ 's for Ni were chosen as the ones obtained through charge interaction for edt and ett complexes of Ni in oxidation states +2 to +4 and then scaled for Fe and Pt.

In tight binding calculations, lattice summations were carried out over two nearest neighbors. Averages over the Brillouin zone were calculated by using sets of special  $k$  points;<sup>85</sup> a set of 10  $k$  points was used for linear systems and the 16  $k$  points sets of Cunningham<sup>86</sup> for the two-dimensional cases.

**Registry No.** ett, 78906-82-8;  $\text{Ni}(\text{edt})_2$ , 19042-52-5;  $[\text{Ni}(\text{edt})_2]_2$ , 98015-46-4;  $\text{Pt}(\text{edt})_2$ , 66906-50-1;  $\text{Ni}(\text{ett})$ , 88205-49-6;  $\text{Ni}(\text{ox})$ , 10345-27-4;  $\text{Ni}(\text{ox})(\text{NH}_3)_2$ , 98015-47-5;  $\text{Ni}(\text{ttsq})$ , 74478-15-2;  $\text{Fe}_4(\text{ett})\text{H}_{12}^{8-}$ , 98015-48-6;  $\text{Ni}_2(\text{ett})\text{H}_4^{4+}$ , 98015-49-7;  $\text{Pt}(\text{ett})_3^{4+}$ , 98015-50-0; S, 7704-34-9; Ni, 7440-02-0; Pt, 7440-06-4.

(81) Keszler, D.; Ibers, J. A. *J. Solid State Chem.* **1984**, *52*, 73.

(82) Hoffmann, R. *J. Chem. Phys.* **1963**, *39*, 1397.

(83) Ammeter, J. H.; Bürgi, H.-B.; Thibault, J. C.; Hoffmann, R. *J. Am. Chem. Soc.* **1978**, *100*, 3686.

(84) Whangbo, M.-H.; Hoffmann, R. *J. Am. Chem. Soc.* **1978**, *100*, 6093.

(85) (a) Pack, J. D.; Monkhorst, H. J. *Phys. Rev. B* **1977**, *16*, 1748. (b) Evarestov, R. A.; Smirnov, V. P. *Phys. Status Solidi* **1983**, *119B*, 9.

(86) Cunningham, S. L. *Phys. Rev. B* **1974**, *10*, 4988.